AFRL-SN-RS-TR-2001-146 Vol II (of VI)
Final Technical Report
July 2001

KNOWLEDGE BASE APPLICATIONS TO ADAPTIVE SPACE-TIME PROCESSING, VOLUME II: AIRBORNE RADAR FILTERING

ITT Systems

Syracuse Research Corporation

Harvey Schuman

APPROVED FOR PUBLIC RELEASE; DISTRIBUTION UNLIMITED.

AIR FORCE RESEARCH LABORATORY
SENSORS DIRECTORATE
ROME RESEARCH SITE
ROME, NEW YORK

This report has been reviewed by the Air Force Research Laboratory, Information Directorate, Public Affairs Office (IFOIPA) and is releasable to the National Technical Information Service (NTIS). At NTIS it will be releasable to the general public, including foreign nations.

AFRL-SN-RS-TR-2001-146 Vol II (of VI) has been reviewed and is approved for publication.

APPROVED: Michael C Wicks

MICHAEL C. WICKS
Project Engineer

FOR THE DIRECTOR: Robert G. Polce

ROBERT G. POLCE, Chief
Rome Operations Office
Sensors Directorate

If your address has changed or if you wish to be removed from the Air Force Research Laboratory Rome Research Site mailing list, or if the addressee is no longer employed by your organization, please notify AFRL/SNRT, 26 Electronic Pky, Rome, NY 13441-4514. This will assist us in maintaining a current mailing list.

Do not return copies of this report unless contractual obligations or notices on a specific document require that it be returned.

REPORT DOCUMENTATION PAGE	Form Approved OMB No. 0704-0188

1. AGENCY USE ONLY *(Leave blank)*	2. REPORT DATE	3. REPORT TYPE AND DATES COVERED
	JULY 2001	Final Aug 95 - Jul 99

4. TITLE AND SUBTITLE
KNOWLEDGE BASE APPLICATIONS TO ADAPTIVE SPACE-TIME PROCESSING, VOLUME II: AIRBORNE RADAR FILTERING

5. FUNDING NUMBERS
C - F30602-95-C-0041
PE - 62702F
PR - 4506
TA - 11
WU - 2B

6. AUTHOR(S)
Harvey Schuman

7. PERFORMING ORGANIZATION NAME(S) AND ADDRESS(ES)
Prime: ITT Systems
775 Daedalian Drive
Rome New York 13441

Sub: Syracuse Research Corporation
6225 Running Ridge Road
North Syracuse New York 13211

8. PERFORMING ORGANIZATION REPORT NUMBER
N/A

9. SPONSORING/MONITORING AGENCY NAME(S) AND ADDRESS(ES)
Air Force Research Laboratory/SNRT
26 Electronic Pky
Rome New York 13441-4514

10. SPONSORING/MONITORING AGENCY REPORT NUMBER
AFRL-SN-RS-TR-2001-146
Vol II (of VI)

11. SUPPLEMENTARY NOTES
Air Force Research Laboratory Project Engineer: Michael C. Wicks/SNRT/(315) 330-2556

12a. DISTRIBUTION AVAILABILITY STATEMENT
APPROVED FOR PUBLIC RELEASE; DISTRIBUTION UNLIMITED.

12b. DISTRIBUTION CODE

13. ABSTRACT *(Maximum 200 words)*

There are many variations of space-time adaptive processing (STAP) that have been proposed since as far back as the 1960s. Practically all of the variations can be grouped into eight general methods. These methods are described in this report. An interesting discussion on the relative merits of the methods and of STAP in general is also included. Contentions are backed up by results from applying STAP to measured data. The merits identified in this report are used later (Volume III) to derive rules for a knowledge-based space-time adaptive processing system.

14. SUBJECT TERMS
Radar, Algorithms, Signal Processing, Space-Time Adaptive Processing, STAP

15. NUMBER OF PAGES
72

16. PRICE CODE

17. SECURITY CLASSIFICATION OF REPORT	18. SECURITY CLASSIFICATION OF THIS PAGE	19. SECURITY CLASSIFICATION OF ABSTRACT	20. LIMITATION OF ABSTRACT
UNCLASSIFIED	UNCLASSIFIED	UNCLASSIFIED	UL

Table of Contents

List of Figures

List of Figures – Cont'd

List of Figures – Cont'd

Section 1.0
Space Time Adaptive Processing

Syracuse Research Corporation
December, 1997

1.1 Introduction

Conventional airborne radar clutter suppression processing usually is limited to beamforming, Doppler filtering, airborne moving target indicator (AMTI) and displaced phase center antenna (DPCA). Essentially, antenna elements (or subarrays) and pulses are weighted and combined to yield Doppler "bins" in sum and difference beams with ground clutter interference suppressed in each beam/bin combination. With AMTI, a null is placed in that part of the Doppler filter response pattern corresponding to ground clutter within a narrow strip of the antenna mainlobe. With DPCA, pulses and antenna elements (or subarrays) are appropriately combined to effectively null ground clutter throughout most of the mainlobe.

Space/Time Adaptive Processing (STAP) methods, essentially, apply adaptivity to this filtering process. The potential effectiveness of deterministic methods, e.g., DPCA and AMTI, is limited by the unknowns associated with antenna errors, receiver mismatch and instability, and platform motion uncertainty. STAP automatically "corrects," within limits, for such unknowns. STAP also suppresses jamming and other radiative interference simultaneously along with clutter. There are many variations of STAP that have been proposed since as far back as the late 1960s. Practically all of the variations can be grouped into eight general methods. The methods are described here. An interesting discussion on the relative merits of the methods and of STAP in general is included, as well. Contentions are backed up by results from applying STAP to measured data.

1.2 STAP Methods

The eight general STAP methods are

1. Factored
2. Element Space Post Doppler ADPCA
3. Element Space Pre-Doppler ADPCA
4. Beam Space Post Doppler ADPCA
5. Beam Space Pre-Doppler ADPCA
6. Joint Domain Localized
7. SLC Post Doppler ADPCA (Σ,Δ & Subarrays Post Doppler)
8. SLC Pre-Doppler ADPCA (Σ,Δ & Subarrays Pre-Doppler)

The term "ADPCA" refers to "adaptive DPCA." This term occasionally is dropped from the method references in the descriptions that follow. The term "SLC" refers to "sidelobe cancellation." The SLC ADPCA methods (7 and 8) sometimes are referred to as "Σ,Δ & Subarrays" methods. Element Space Post Doppler ADPCA (Method 2) is referred to in the literature, occasionally, as "PRI Staggered."

Block diagrams for the STAP methods are given, respectively, in Figures 1-1 through 1-8. Preadaptive complex data samples are denoted by x and post adaptive complex samples by y (lower case for pre-Doppler and upper case for post Doppler), N_s = number of spatial (element, subarray, or beam) channels, N_t = number of pulses in the CPI, K_s = number of STAP spatial degrees of freedom, K_t = number of STAP temporal degrees of freedom, and the adaptive weights are denoted by w. Although only two temporal channels (one pulse delay between them) per spatial channel are shown in the diagrams for all methods except 1 and 6, any number of temporal channels between 0 and the number of pulses in the CPI actually can be applied in the corresponding method. Typically these temporal channels are restricted to being separated by one pulse delays, as shown. If only one temporal channel per spatial channel is specified, Element Space Post Doppler (Method 2) is identical to Factored STAP (Method 1). Factored STAP is identified as a separate method for convenience because of its common usage.

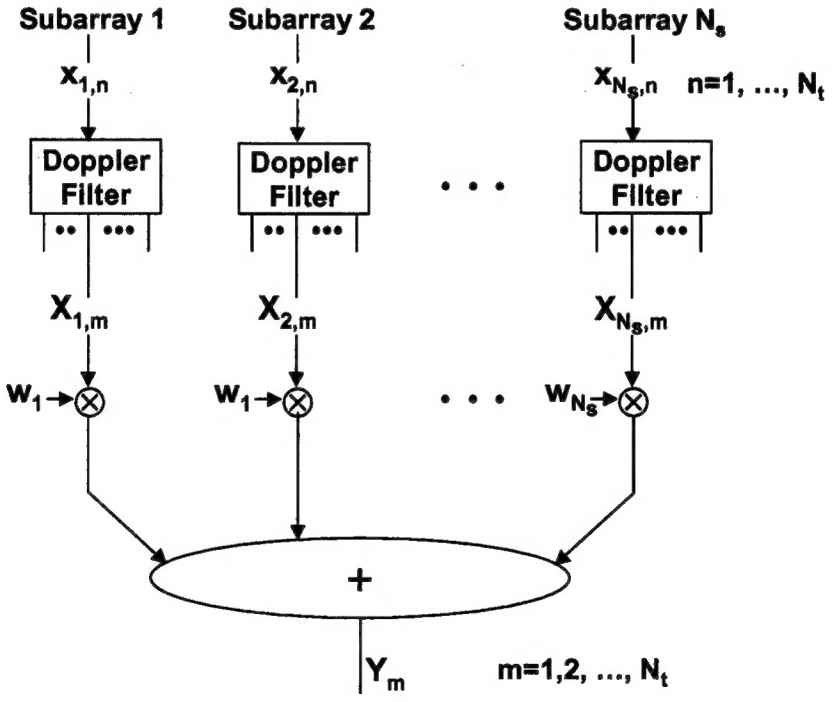

Figure 1-1: Factored STAP

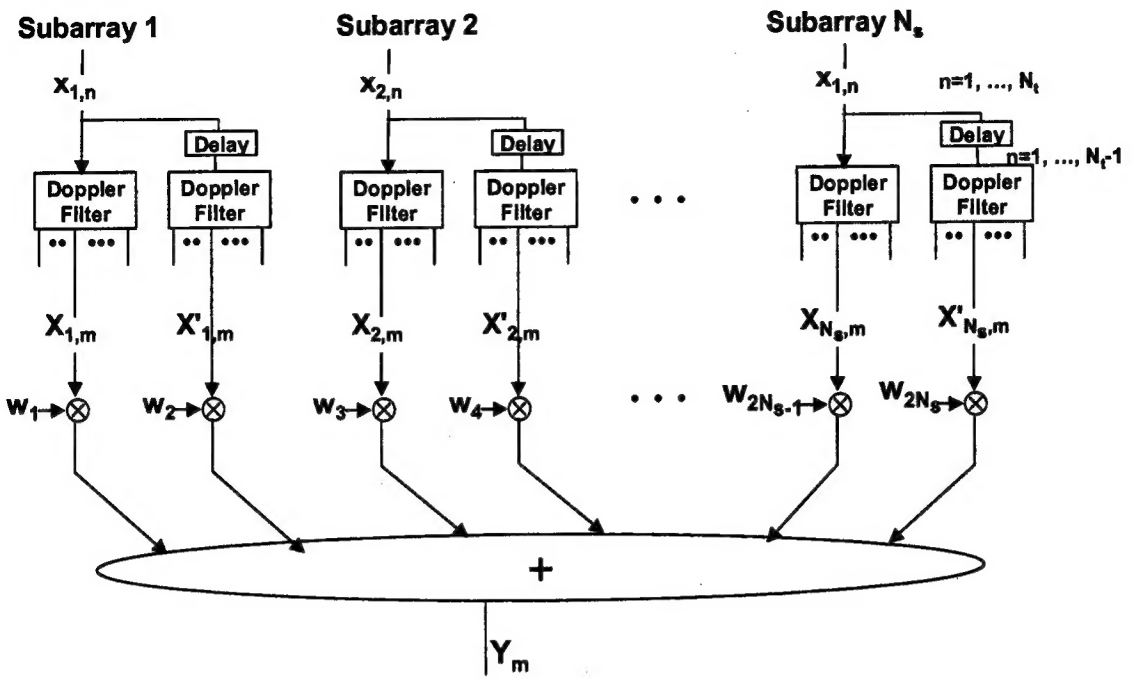

Figure 1-2: Element Space Post-Doppler STAP

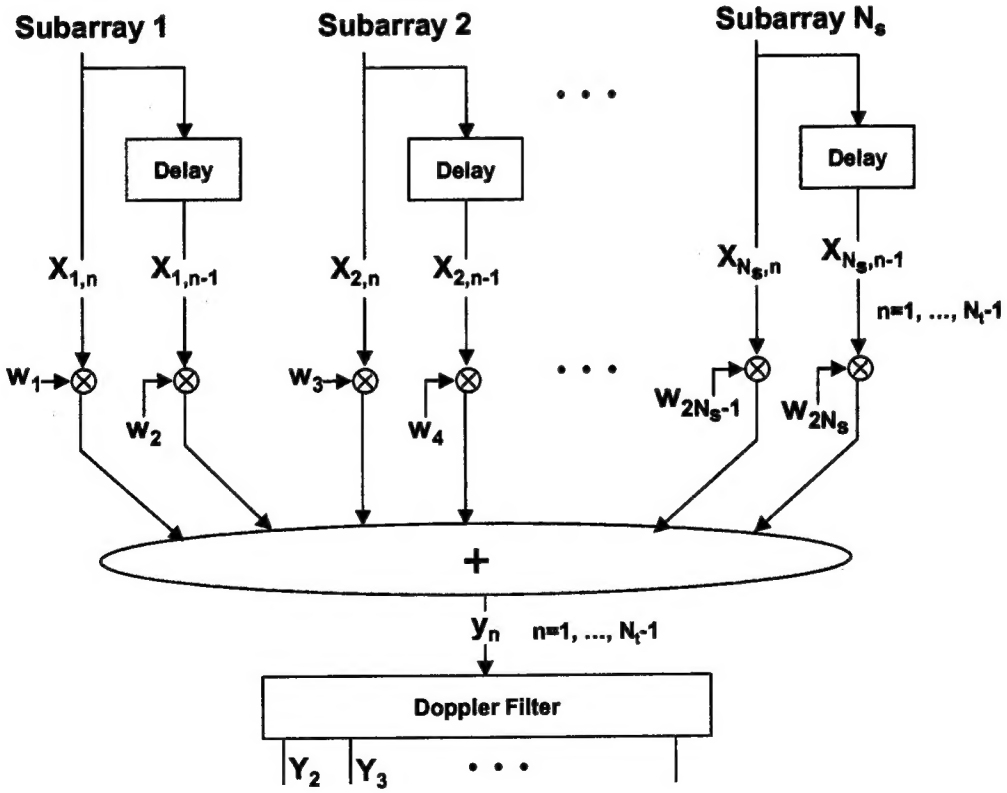

Figure 1-3: Element Space Pre-Doppler STAP

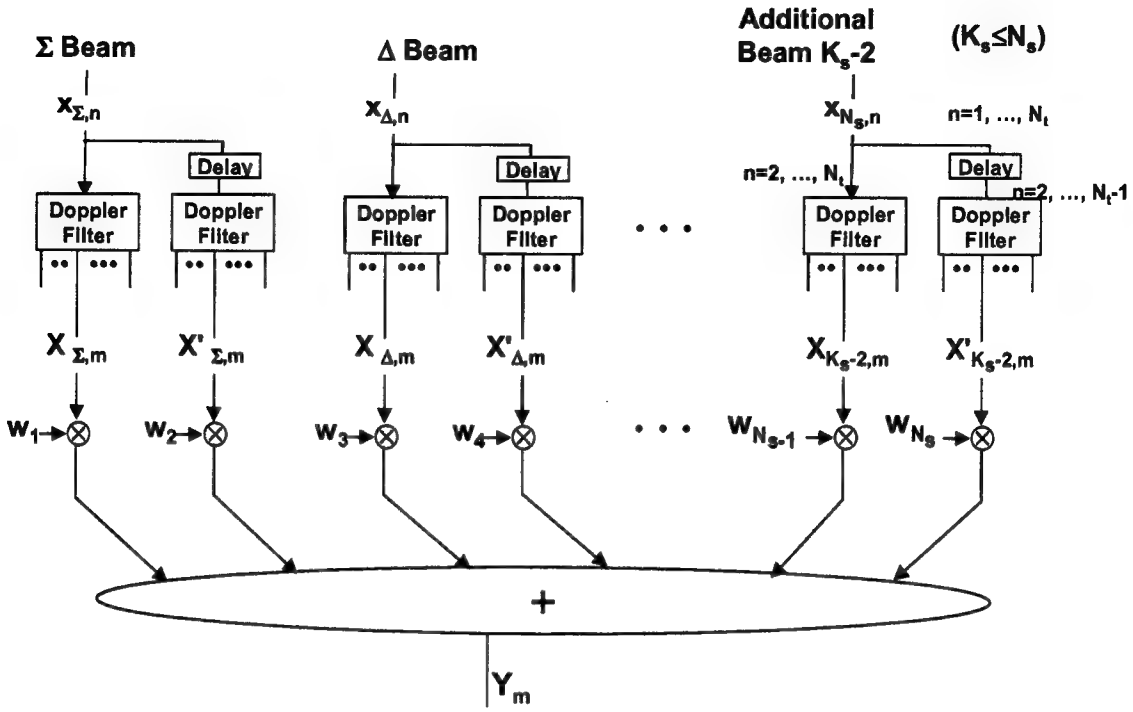

Figure 1-4: Beam Space Post-Doppler STAP

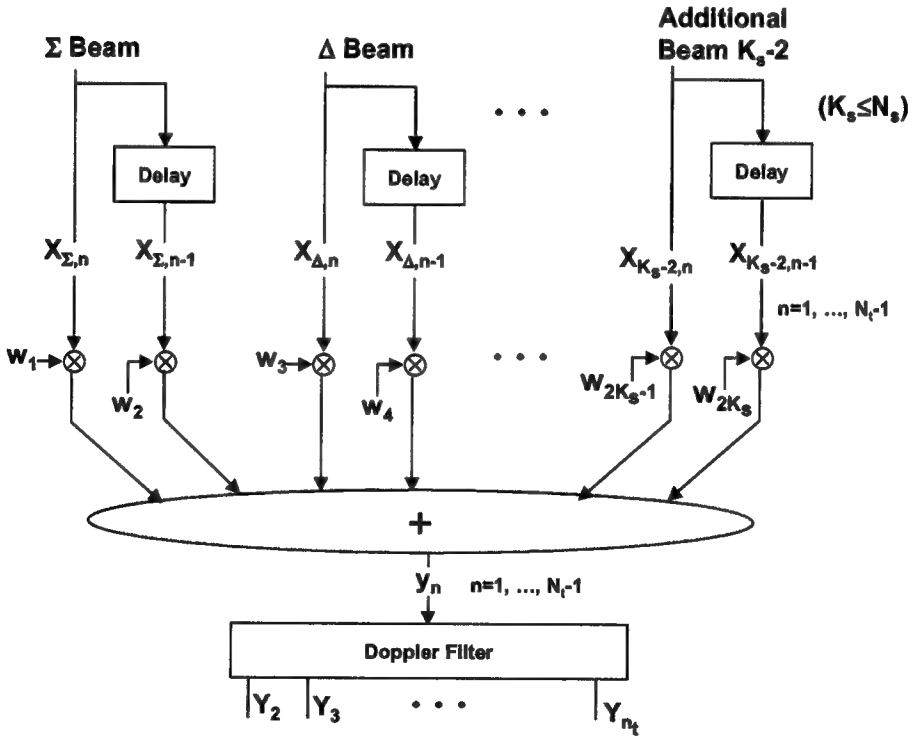

Figure 1-5: Beam Space Pre-Doppler STAP

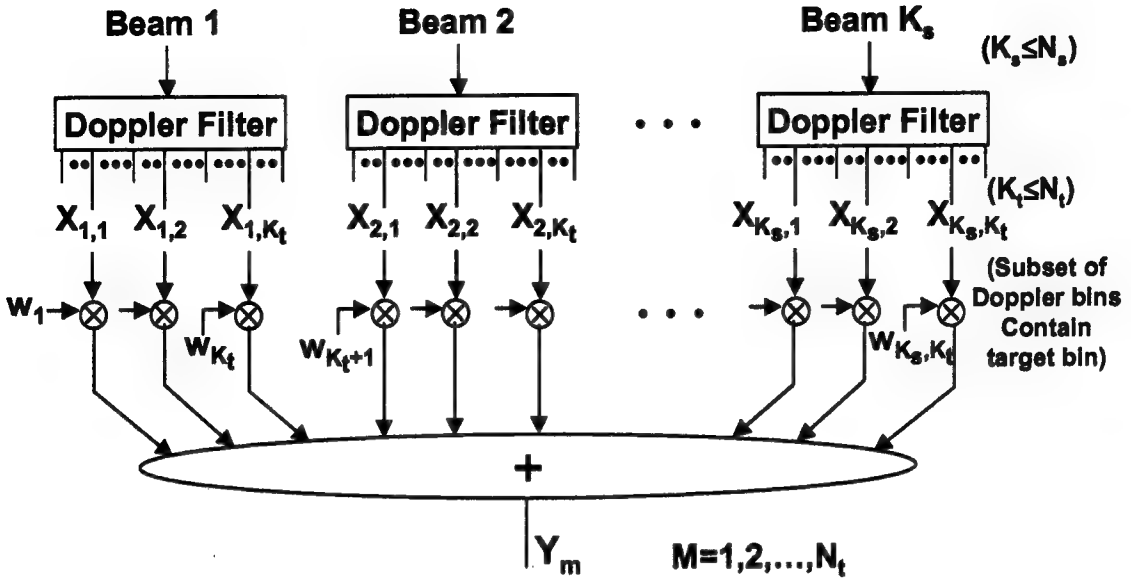

Figure 1-6: Joint Domain Localized STAP

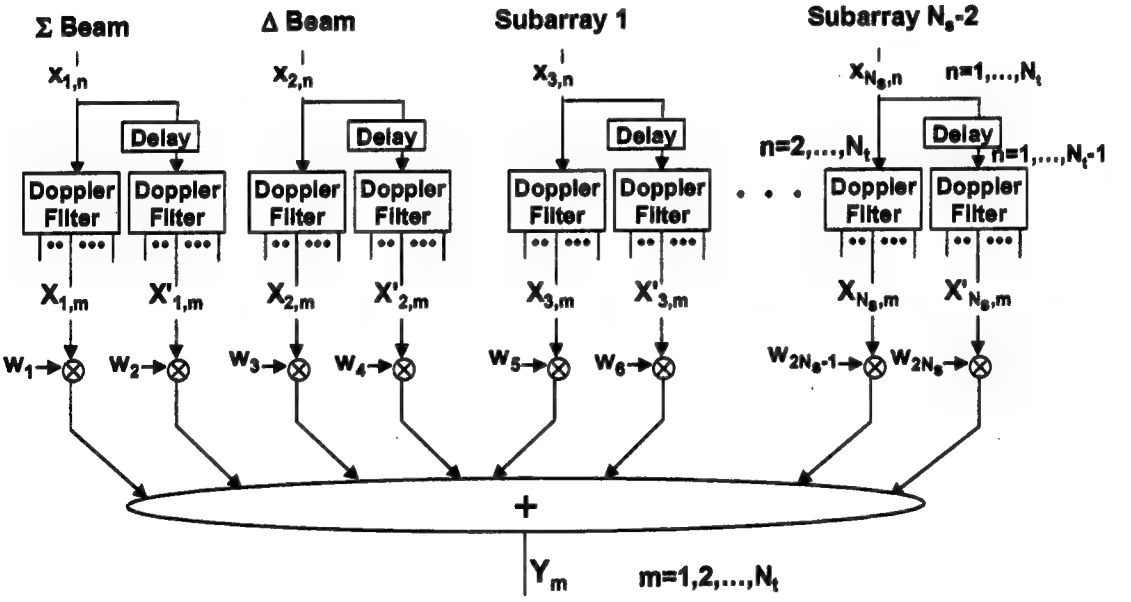

Figure 1-7: SLC Post-Doppler STAP

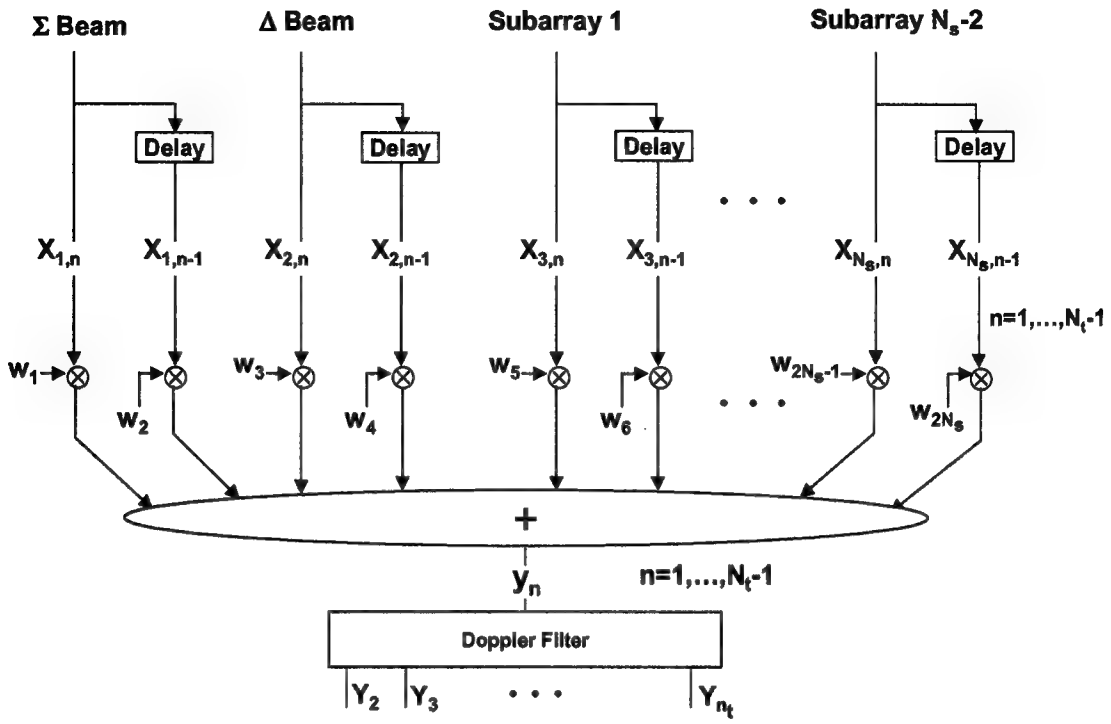

Figure 1-8: SLC Pre-Doppler ADPCA STAP

In Factored STAP, as it is defined here, first, the pulses associated with each subarray channel are passed through a Doppler filter. Spatial adaptivity then is applied to all corresponding resolution cell ("bin") outputs of the Doppler filters. Factored STAP, it is occasionally argued, is not truly STAP because the adaptivity is performed in the spatial domain only and not the combined space/time domain. It is essential that the adaptivity not precede the Doppler filtering and that the latter be heavily weighted for low sidelobes. This ordering and low sidelobe weighting is important because the clutter that must be suppressed by adaptivity then would principally originate from confined angular regions (portions of the "clutter ridge" intercepted by the Doppler mainlobe and, possibly, ambiguity lobes) and thus would be manageable with the number of degrees of freedom (N_{DOF}) limited to the number of spatial channels. The number of degrees of freedom is defined here as the product of the spatial channels (or beams) and pulses (or Doppler bins) applied in the STAP. The STAP covariance matrix, used to obtain the adaptive weights, generally is of order N_{DOF}. (An exception occurs when mainlobe constraints are applied, as described in a subsection below.)

Also, Factored STAP as defined here perhaps is more appropriately referred to as "Time/Space Factored STAP" to reflect the ordering of the operations (Doppler filtering [temporal] followed by adaptive beamforming [spatial]). Another form of "Factored STAP," appropriately referred to as "Space/Time Factored STAP," is characterized by adaptively combining the pulses associated with the output of a (spatial) beamformer such as a sum or difference channel output. One might suspect that Time/Space Factored is superior to Space/Time

Factored when the CPI contains a large number of pulses (narrow Doppler filter) and the reverse is true when the array is large (narrow beams) and well controlled for low sidelobes. For those systems where the CPIs and arrays both are large and well controlled, there may be little benefit that can be provided by any STAP method. In fact, simulation suggests that STAP provides minimal improvement for such systems.

Joint Domain Localized (JDL) refers to processing whereby Doppler bins and spatial beams are adaptively combined. Several combinations of beams and bins have been explored using sum and difference channels and digitally formed beams. It has been found through extensive simulation that a particularly effective JDL configuration is that which employs three Doppler bins (the target [or "test"] bin and immediate adjacent bins) and four beams (target sum and difference beams and immediate adjacent sum beams).

Adaptive DPCA (ADPCA) methods (Methods 2,3,4,5,7, and 8) refer to processing whereby a subset of successive samples (sometimes referred to as a "sub-CPI") from all spatial channels are adaptively combined. The channels can be beams (beam space) or subarrays (element space) and the samples either pulses (pre-Doppler) or Doppler bins (post Doppler). It is interesting to compare JDL with Beam Space Post Doppler ADPCA. Whereas both methods are characterized as "post Doppler beam space and small $N_{DOF,}$" JDL is quite different from Post Doppler Beam Space ADPCA. With JDL, *one* Doppler filter is applied to each of several adjacent beam channels and *several* adjacent Doppler frequency bins from each filter are combined adaptively with the corresponding bins from all the filters. With Post Doppler Beam Space ADPCA, *several* Doppler filters are applied to each beam channel, the filters differing by an n-pulse delay applied to the pulse stream they operate on, and *one* corresponding Doppler bin from all the filters are adaptively combined. The point here is that JDL combines several Doppler bins (frequencies) in generating adaptive weights, whereas ADPCA uses only one bin (the target bin) from Doppler filters that operate on delayed pulse streams to effect a DPCA condition. JDL, on the other hand, can be viewed as a two-dimensional (space/time) sidelobe canceller.

The pre-Doppler ADPCA methods can be implemented wherein only one set of adaptive weights are computed for the entire CPI. The weights computed using the first sub-CPI are reapplied for all successive sub-CPIs. This implementation is computationally efficient. Its effectiveness may deteriorate if intrinsic clutter motion is especially severe and/or receiver pulse to pulse stability is an issue. In such cases, a more computationally demanding implementation, recomputation of the weights for each sub-CPI, would be of value.

Post Doppler (or Pre-Doppler) "Sidelobe Canceler (SLC)" STAP refers to an ADPCA type of method with the inclusion of both beams and subarrays as spatial degrees of freedom in the adaptive procedure. The beams are typically the sum and difference beams and so this STAP method also is referred to as "Σ,Δ & Subarrays STAP." These methods have been found, through limited simulation, to be particularly effective.

1.3 Covariance Matrix Estimation

The STAP methods often are applied in a weight generation/application procedure. Here, adaptive weights are determined according to $\boldsymbol{w} = \boldsymbol{R}^{-1}\boldsymbol{s}$ where $\boldsymbol{R}$ is the interference covariance

matrix and $\boldsymbol{s}$ is the steering vector. This expression would result in weights that maximize signal to interference plus noise ratio (SINR) if $\boldsymbol{R}$ and $\boldsymbol{s}$ are known exactly. The steering vector typically is chosen to be the combiner weights that would be applied in a corresponding nonadaptive processor; e.g., in element (or subarray) space methods the steering vector is phased according to the target direction and Doppler and, perhaps, amplitude weighted for low angle/Doppler sidelobes. The optimum steering vector phasing is not known exactly because of antenna and receiver errors. Also, the covariance matrix is, at best, only estimated from reference data corresponding to range cells other than the target (test) cell and immediate neighboring cells (guard cells).

For post pulse compression STAP, a sliding window method of reference data selection, for STAP weight generation, is often applied. The reference data is obtained from range cells neighboring the test cell but exclusive of "guard" cells immediately surrounding the test cell. A recommended number of reference cells is $2N_{DOF}$. Note that the weights must be recomputed for each test range cell. (They are recomputed for each test Doppler cell, as well, in some STAP methods.) The purpose of the guard cells is to help prevent "mainlobe" gain loss in the adaptive process that results from target response signal influencing weight generation. (Additional considerations regarding mainlobe gain loss are discussed below in subsections on diagonal loading and mainlobe constraints.)

For precompression STAP, a fixed window method of reference data selection is reasonable. Here, the same weight vector is applied to all test range cells. If the range extent is not too large (limited, perhaps, to hundreds of cells), data from all range cells might be included in the reference data. Otherwise, one might limit the number of reference data range cells to the product of $2N_{DOF}$ and the pulse compression ratio, i.e., the number of cells traversed by the precompressed pulse. The rationale for the latter rule is that $2N_{DOF}$ *independent* samples generally is adequate for estimating the covariance matrix and the precompressed pulse is roughly correlated over a number of cells given by the compression ratio.

1.4 Diagonal Loading

A minimum amount of diagonal loading may be desirable to prevent target signal suppression (mainlobe gain loss) in the STAP process regardless of the processing architecture. A rule for determining the minimum amount requires estimating the minimum signal to noise level at the element (subarray or column) output prior to pulse compression and Doppler processing (SNR_e). This value can be estimated from the radar parameters, test range cell (R_t), and minimum target cross section (σ_t) in accordance with the radar range equation. With SNR_e estimated, the minimum amount of diagonal loading can be determined as a function of the order of processing. Consider the following definitions:

PCR = pulse compression ratio (dB)

$PCSL$ = pulse compression sidelobe level (dB)

DNR = minimum diagonal loading (plus noise) to noise ratio (dB); (0 dB $\rightarrow$ 3 dB increase in "noise" in STAP weight generation process)

RGB = receive beamformer gain (dB)

DFG = Doppler filter gain (dB)

The value of DNR depends on the order of processing. Eight possibilities are pertinent. These follow with the associated equation for determining DNR.

1. Pulse compression → Element space STAP → Doppler filtering

   $$DNR = SNR_e + PCR - PCSL$$

2. Pulse compression → Beam space STAP → Doppler filtering

   $$DNR = SNR_e + PCR + RBG - PCSL$$

3. Pulse compression and Doppler filtering → Element space STAP

   $$DNR = SNR_e + PCR + DFG - PCSL$$

4. Pulse compression and Doppler filtering → Beam space STAP

   $$DNR = SNR_e + PCR + DFG + RGB - PCSL$$

5. Element space STAP → Pulse compression and Doppler filtering

   $$DNR = SNR_e$$

6. Beam space STAP → Pulse compression and Doppler filtering

   $$DNR = SNR_e + RBG$$

7. Doppler filtering → Element space STAP → Pulse compression

   $$DNR = SNR_e + DFG$$

8. Doppler filtering → Beam space STAP → Pulse compression

   $$DNR = SNR_e + DFG + RBG$$

1.5 Mainlobe Constraints

Another means of helping limit cancellation of the target response signal in the adaptive process is to filter the target signal from the weight determination process. The advantage of employing this "hard constraint" method is that the resulting adaptive weights generally are not as desensitized to the clutter as they might be if substantial diagonal loading were included in their generation. Greater clutter suppression then is generally possible. The disadvantage is that a small number of the degrees of freedom must be diverted from clutter suppression to filtering. In other words, the order of the covariance matrix is reduced. If the "rank" of significant clutter is equal to or greater than the number of degrees of freedom, diagonal loading may be preferable to mainlobe constraints.

1.6 Discussion

The STAP methods have been applied to Multichannel Airborne Radar Measurement (MCARM) monostatic radar data recently made available through the USAF Rome Laboratory [1]. The goal was to identify rules regarding the relative performance of the methods in suppressing airborne radar clutter. Some results and conclusions derived from this effort are summarized below.

The MCARM antenna is a side mounted array. The array contains 24 combiners on receive. These feed 22 subarray channels, a Taylor weighted Σ channel, and a Bayliss weighted Δ channel. The subarray channels, as configured for monostatic measurements, correspond to two horizontal rows of 11 subarrays each. Each subarray is comprised of four radiating elements aligned in elevation. The rows are displaced in elevation (one directly above the other) by the length of a subarray. The frequency band is L-Band, the range resolution is 120 m, and the coherent processing interval (CPI) contains 128 pulse repetition intervals (PRIs).

For the processing examples discussed here, the aircraft velocity was about 100 m/s and altitude about 10,000 ft. The aircraft motion effected a "crab" angle of 7.28 degrees. The terrain was in the vicinity of the expanse between the Chesapeake Bay and the Delaware River at about the latitude of Baltimore. A target signal was injected into the digitized data channels at range cell 350 and radial velocity (with respect to ground) 20 m/s.

Post Doppler beam space ADPCA methods generally were found to be more effective than pre-Doppler or element space ADPCA methods especially for small N_{DOF}. This observation is supported by the results shown in Figures 1-9 and 1-10 which were obtained by applying Beam Space Pre-Doppler ADPCA and Beam Space Post Doppler ADPCA, respectively, to the MCARM data (Σ and Δ spatial channels only). This observation can be explained as follows. Because with beam space methods usually the number of degrees of freedom is small, adaptivity can not totally compensate for all errors (velocity/PRI mismatch, nonuniform motion, subarray mismatch, crab, etc.) in attempting to realize a DPCA-like suppression filter. These errors can be thought of as broadening and bending the clutter "ridge" in sine angle/Doppler space. Ideally, the ridge is narrow and straight and a DPCA solution exists that nulls the entire ridge. With errors, however, the ridge distorts and small N_{DOF} adaptivity is best applied only to those portions of the ridge that are not otherwise suppressed by Doppler filtering. In other words, with pre-Doppler ADPCA, some clutter that is suppressed adaptively would only have been filtered anyway in the subsequent Doppler processor, but with post Doppler ADPCA, only that clutter that passes through the Doppler processor (usually primarily Doppler mainlobe clutter) would require suppression adaptively. Post Doppler ADPCA, therefore, generally can be expected to be superior to pre-Doppler ADPCA when N_{DOF} is small.

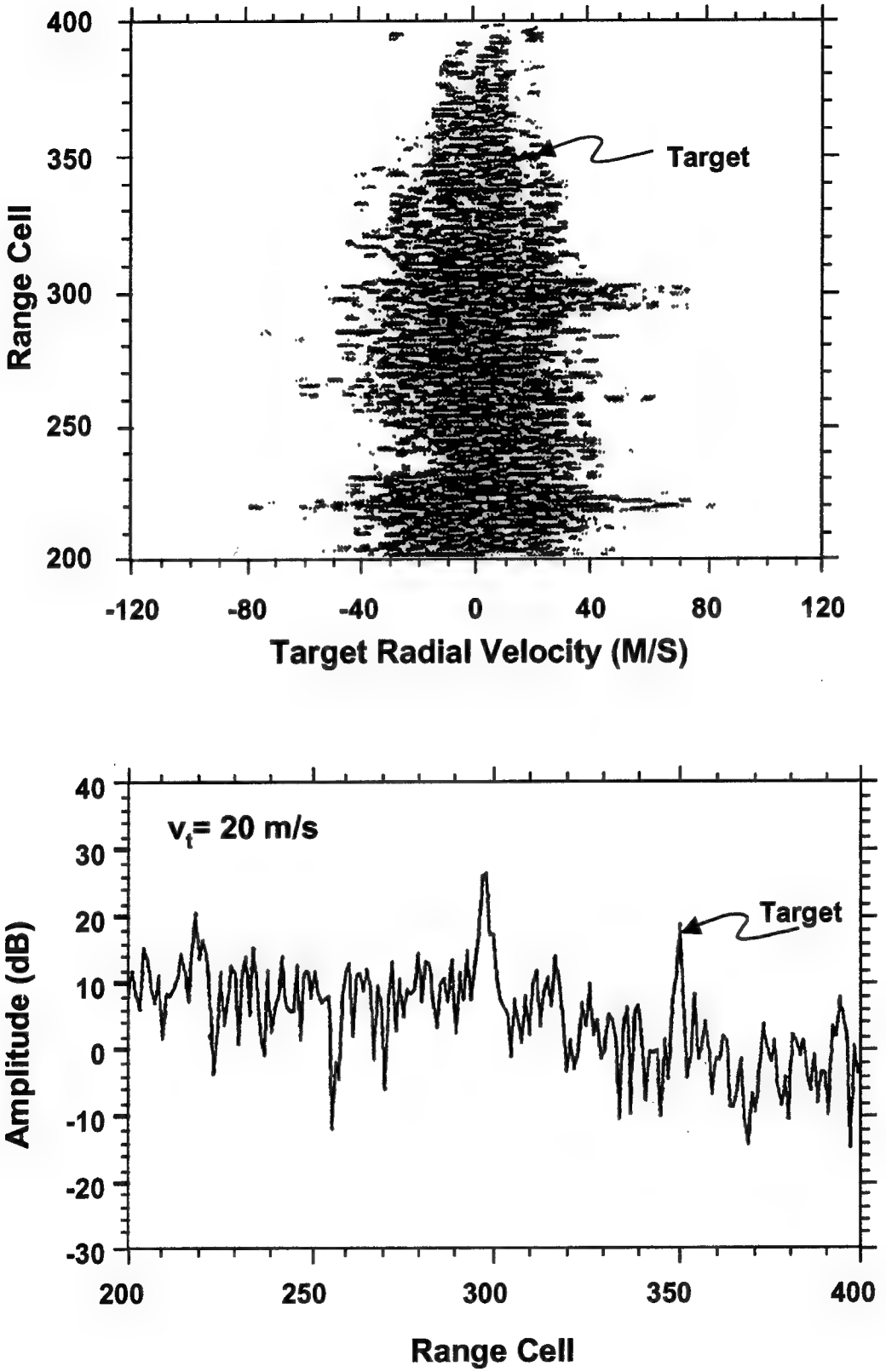

Figure 1-9: Beam Space Pre-Doppler ADPCA Processor Output

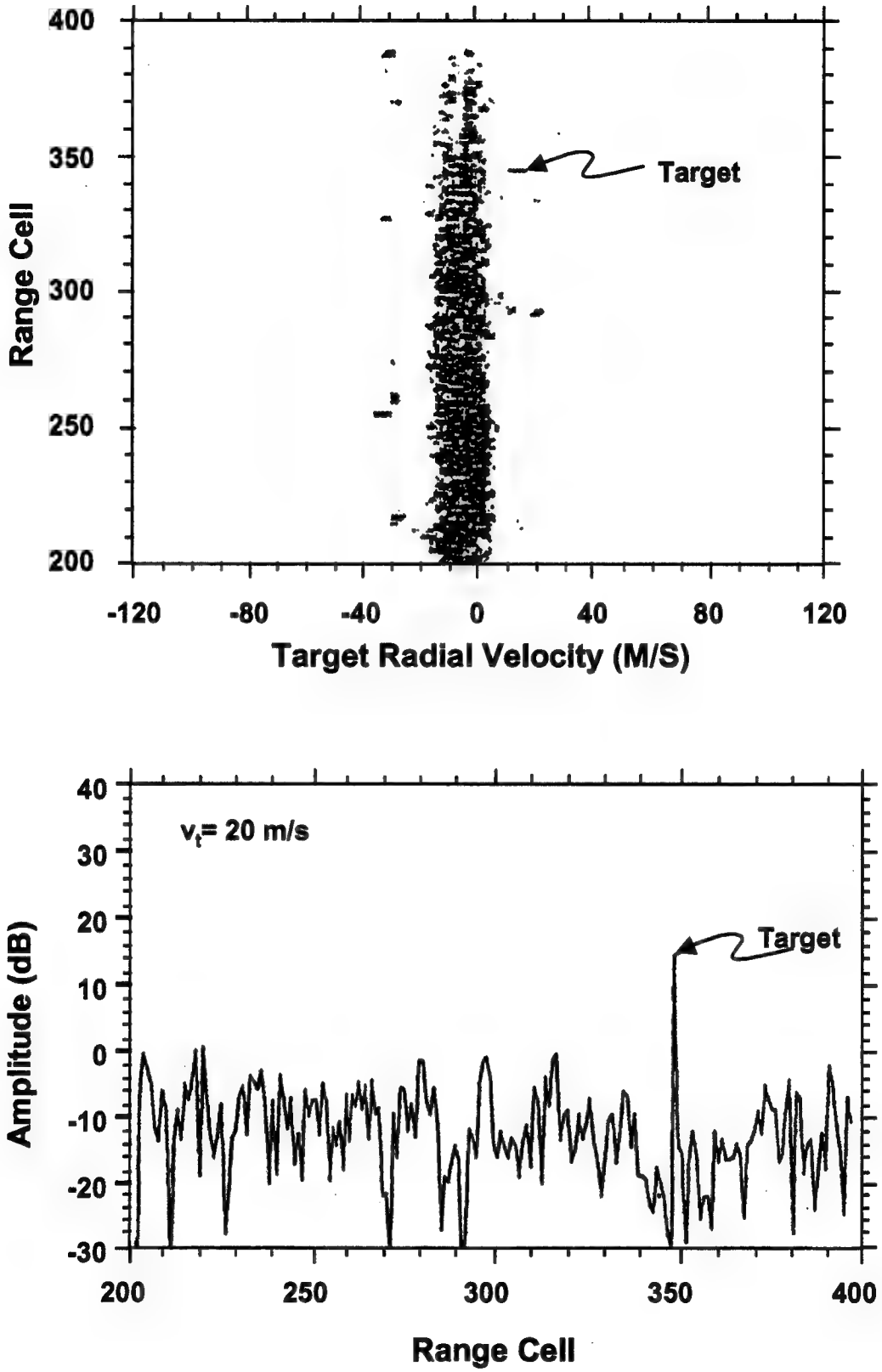

Figure 1-10: Beam Space Post Doppler ADPCA Processor Output

In general, it has been found that Doppler filtering and beamforming, all "deterministic processing," best precede STAP adaptivity. An important underlying assumption to this conclusion is that pulse compression with heavy time sidelobe suppression weighting (in excess of ~ 40 dB) also precede adaptivity. Otherwise, if pulse compression follows STAP, the target SNR is likely to be substantial in the range cells used for weight determination (reference data cells) because of the gain associated with Doppler filtering and beamforming. Substantial target SNR in the reference cells would require that heavy diagonal loading or "hard" mainlobe constraints be applied in weight computation in order to prevent target gain loss in the adaptive process, as indicated by the appropriate relations given in the above subsections on diagonal loading and mainlobe constraints. Thus, it has been found that when STAP precedes pulse compression, STAP performance generally is best if STAP also precedes Doppler filtering. If the only beams formed in the STAP algorithm are Σ,Δ beams, however, and since the Δ channel essentially blocks the target response signal from entering the weight generation process (functioning as a "hard" constraint - see above subsection on mainlobe constraints), perhaps it is not surprising that Σ,Δ & Subarrays ADPCA algorithms (subarray channels generally have relatively low gain) have been found not to degrade too badly with precompression STAP as long as the Doppler filtering is relocated to follow the STAP. (The Joint Domain Localized (JDL) algorithm, for example, has been found to perform especially poorly with precompression STAP.)

It was observed that whereas Factored STAP loses effectiveness if the Doppler filter sidelobe levels rise above the two way antenna gain pattern sidelobe levels, element space ADPCA is actually more effective with the higher Doppler filter sidelobe levels. This observation can be explained as follows. Consider the angle/Doppler diagram of Figure 1-11. This diagram corresponds to the MCARM data at hand: the slight crab angle results in the elliptic shaped clutter ridge, the beamwidth of the indicated two-way antenna pattern is roughly that of the MCARM antenna, and the width of the Doppler filter indicated is roughly that of the MCARM filter, as well. Two regions of principal sources of clutter are shown in the angle/Doppler diagram. One region, denoted "A", lies within the intersection of the clutter ridge with the antenna mainlobe and the Doppler filter sidelobes. The second region, denoted "B", lies within the intersection of the clutter ridge with the Doppler filter mainlobe and the antenna sidelobes. The spatial adaptivity component of factored STAP is ineffective against Region A clutter. Nulled regions resulting from this adaptivity would appear as horizontal ribbons in the diagram. Region A clutter, therefore, cannot be suppressed with spatial only adaptivity without severe loss in mainlobe gain. Factored STAP thus relies on low Doppler sidelobes to suppress Region A clutter. If the Doppler sidelobe level exceeds the two way antenna sidelobe level, Region A clutter would likely dominate and Factored STAP would be expected to lose effectiveness.

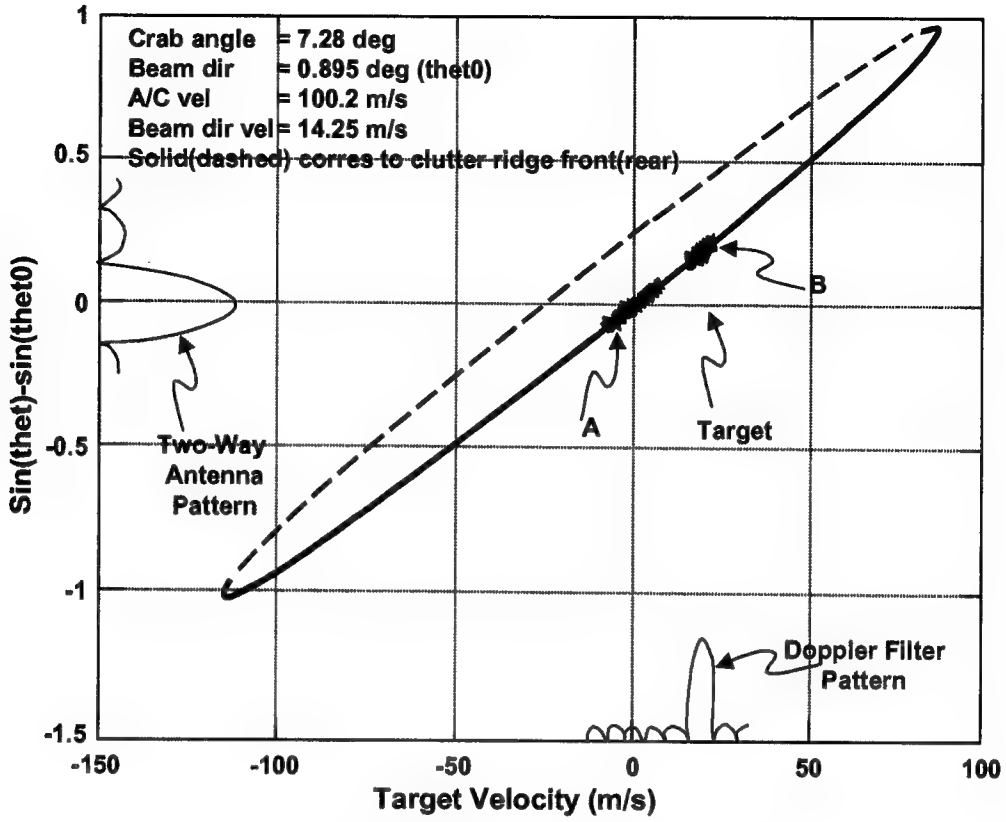

Figure 1-11: Angle/Doppler Diagram

ADPCA on the other hand, would be effective in adaptively suppressing both Region A and Region B clutter because, with ADPCA, nulls are formed close to and nearly parallel to the clutter ridge. Consequently, low Doppler filter sidelobes may not be necessary for ADPCA, and, in fact, may be a detriment because of the associated loss in Doppler filter gain. (This conclusion does not necessarily apply to small N_{DOF} ADPCA such as Beam Space ADPCA.) Verification of this assertion is evident from the MCARM data. The peak two-way antenna sidelobes are roughly -50 dB. One, then, would expect Region A clutter to dominate when the Doppler sidelobe level exceeds about -50 dB. The signal to interference plus noise ratio (SINR) is shown in Figure 1-12 for Factored STAP (solid) and Element Space Post Doppler ADPCA (dashed) as functions of Doppler filter sidelobe weighting. Factored STAP appears to perform best with Doppler filter sidelobes below about -50 dB and ADPCA appears to perform best with filter sidelobes above about -50 dB, as is consistent with the assertion. Mainlobe gain loss (target response loss due to processing) is shown in Figure 1-12, as well. Factored STAP experiences severe loss for higher Doppler filter sidelobe levels as would be expected because of the corresponding dominance of Region A clutter. ADPCA, on the other hand, experiences several dB less loss with higher filter sidelobes over that with lower sidelobes as would be expected because of the reduced filter mainlobe gain loss associated with higher sidelobes.

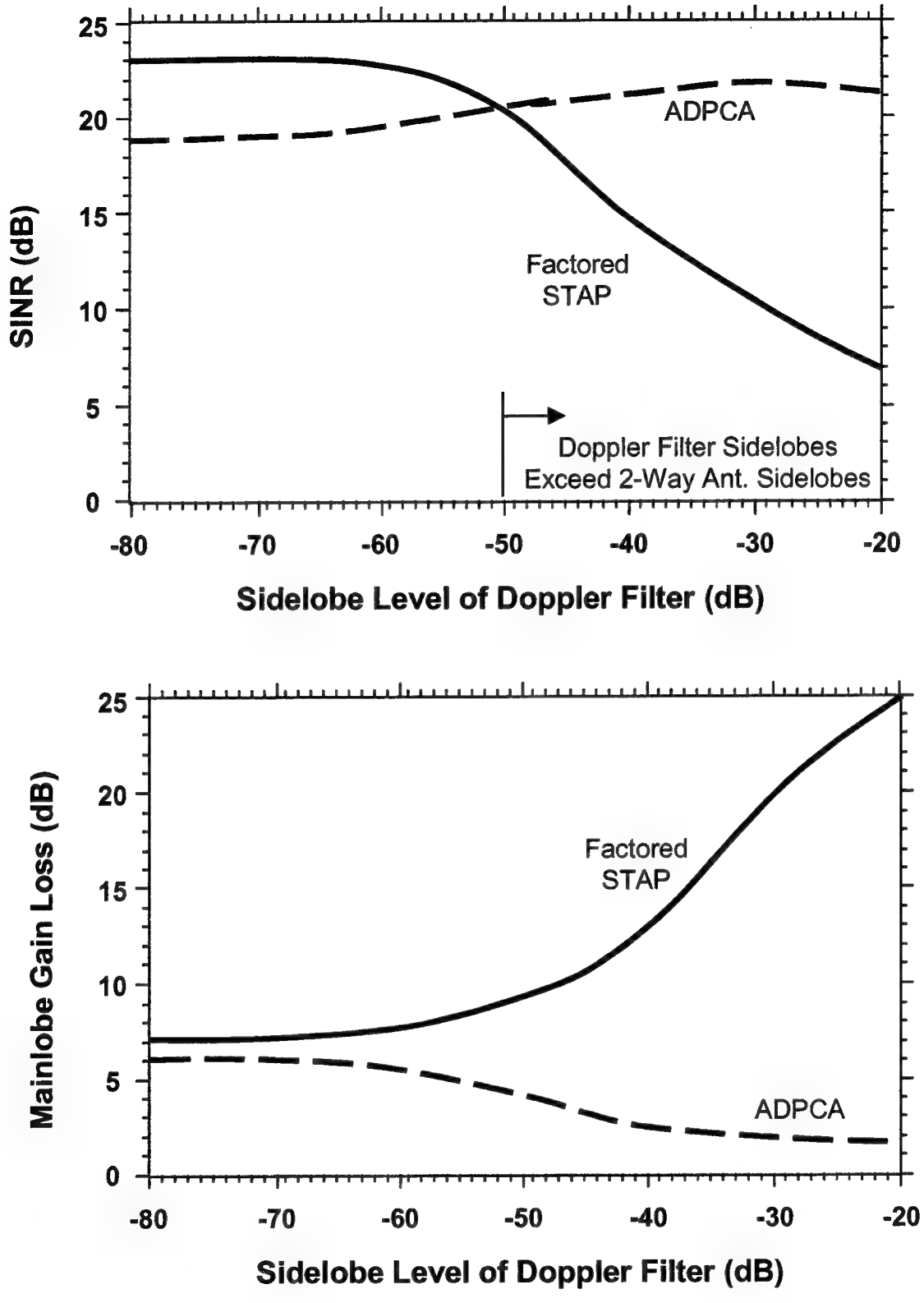

Figure 1-12: STAP Method Comparison

As a final note, it is interesting to observe that a variant of Beam Space Pre-Doppler STAP, one in which the sum and difference beams comprise the spatial degrees of freedom and referred to here as "Σ&Δ ADPCA," was introduced and extensively studied over 25 years ago by Syracuse Research Corporation (Applebaum, et. al.) [2] as a compliment to the element space ("fully adaptive") approach proposed by Technology Services Corporation (Brennan, et. al.) [3]. Only analog implementations of both approaches were considered at the time. Two advantages of Σ&Δ ADPCA over the fully adaptive approach were identified as 1. reduced complexity (for an AWACS size aperture and CPI, hundreds of degrees of freedom are required for element space ADPCA in contrast with only 3 to 5 degrees of freedom for Σ&Δ ADPCA), and 2. associated reduced settling times (analog implementation). It appears, therefore, that the only recent developments in Σ&Δ ADPCA are the introduction of digital implementation and post Doppler processing. The reduced settling time advantage of beam space over element space when considering analog implementations is equated to reduced number of reference data vectors when considering digital implementations.

Section 1.0 References

1. "Multichannel Airborne Radar Measurement (MCARM) " Final Report, Volume 1 (MCARM Flight Test), AF Contract F30602-92-C- 0161, September 1995.

2. S. P. Applebaum, et. al., "Adaptive Array Antennas," Syracuse University Research Corporation, SRC TR71-137R, 31 May 1971

3. D. L. Ringwalt, et. al., "Adaptive Array Flight Definition Study," NRL Report 7695, AD528643, 21 December 1973.

Section 2.0
Subarray/Sub-CPI Nulling

Syracuse Research Corporation
January 6, 1998

2.1 Introduction

Antenna architectures containing a large number of receivers, perhaps one receiver per column array, are candidates for digital filtering at the subarray level. The subarrays can be weighted to yield radiation patterns with nulls in intense interference directions such as angles corresponding to ground scattering at radial velocities centered within the Doppler filter. The subarray weights can be recomputed for each Doppler filter. The subarrays must overlap to ensure that the subarray apertures are large enough to provide the desired nulling with minimal mainlobe gain loss and that the number of subarrays are large enough to form an array factor with desired sidelobe level and beamwidth. Overlapping is easily realized with digital subarray combining in contrast with analog subarray combining because, with analog combining, extensive hardware is required and severe mutual coupling issues must be addressed.

With this architecture, spatial processing mirrors "Airborne MTI" temporal processing. Subarrays in space and "sub-CPIs" in time can be formed with identical logic, each applied to filtering a different space/time dimension. Or, the subarray and sub-CPI weights can be determined simultaneously to yield a null along the clutter ridge. Also, the array factor weights and "CPI factor" weights, denoting the corresponding means of combining subarrays and sub-CPIs, can be determined from identical logic that optimizes the trade between mainlobe width and sidelobe level in each dimension.

Subarray/sub-CPI filtering is reviewed in the following subsection. Following that, an iterative method for determining the optimum sizes of the subarrays and sub-CPIs is summarized. This method forms the basis of two knowledge base controller rules for deterministic filtering (Rules 1 and 2 in Reference 1). The aim of the methods is to suppress mainlobe clutter (in space and in time) to the array factor and CPI factor sidelobe levels within the constraint of maintaining a minimum signal to noise ratio. An example of the application of the rules is given in the concluding subsection.

Recently, a variation of Rule 1 has been investigated that may prove superior to that report in Reference 1. In this variation, the subarrays and sub-CPIs are sized to maximize an estimate of signal to clutter ratio within the constraint of maintaining a minimum signal to noise ratio. This attractive variant is discussed in the example subsection below.

The impact of limited processing power has not been addressed to date in the development of the subarray/sub-CPI nulling filter. In practice, it may be necessary to divide the range/Doppler window into segments and to apply the filter determined at the center of a segment to all range/Doppler resolution cells within that segment, rather than to recomputed the filter for each range/Doppler resolution cell.

2.2 Filtering

Consider the angle/Doppler diagram of Figure 2-1. A typical array factor, CPI factor, subarray pattern, and sub-CPI pattern are shown plotted in their respective domains by solid lines. The dashed patterns correspond to subarray and sub-CPI patterns mapped into their opposing domains; i.e., the subarray pattern is plotted in Doppler space via mapping through the clutter ridge, and the sub-CPI pattern is plotted in angle space via mapping through the clutter ridge. The point of this display is to emphasize the function of the subarrays and sub-CPIs: the subarrays and sub-CPIs are steered and weighted so that they independently null ground clutter in the angle and Doppler mainlobes. For the filtering considered here, the subarrays and sub-CPIs are formed deterministically and the array factor and CPI factor are formed either deterministically or, if conditions permit, adaptively (STAP). The subarrays and sub-CPIs are phased to steer nulls in the appropriate directions, in angle (subarray) and Doppler (sub-CPI), and a binomial amplitude weighting is applied in each case. The subarray and sub-CPI sizes [number of elements (or columns) and pulses, respectively], and, consequently, null widths, are determined in accordance with the desire to suppress as much mainlobe clutter as possible without suffering unacceptable processing loss. The null widths are suggested in Figure 2-1 by the vertical and horizontal ribbons.

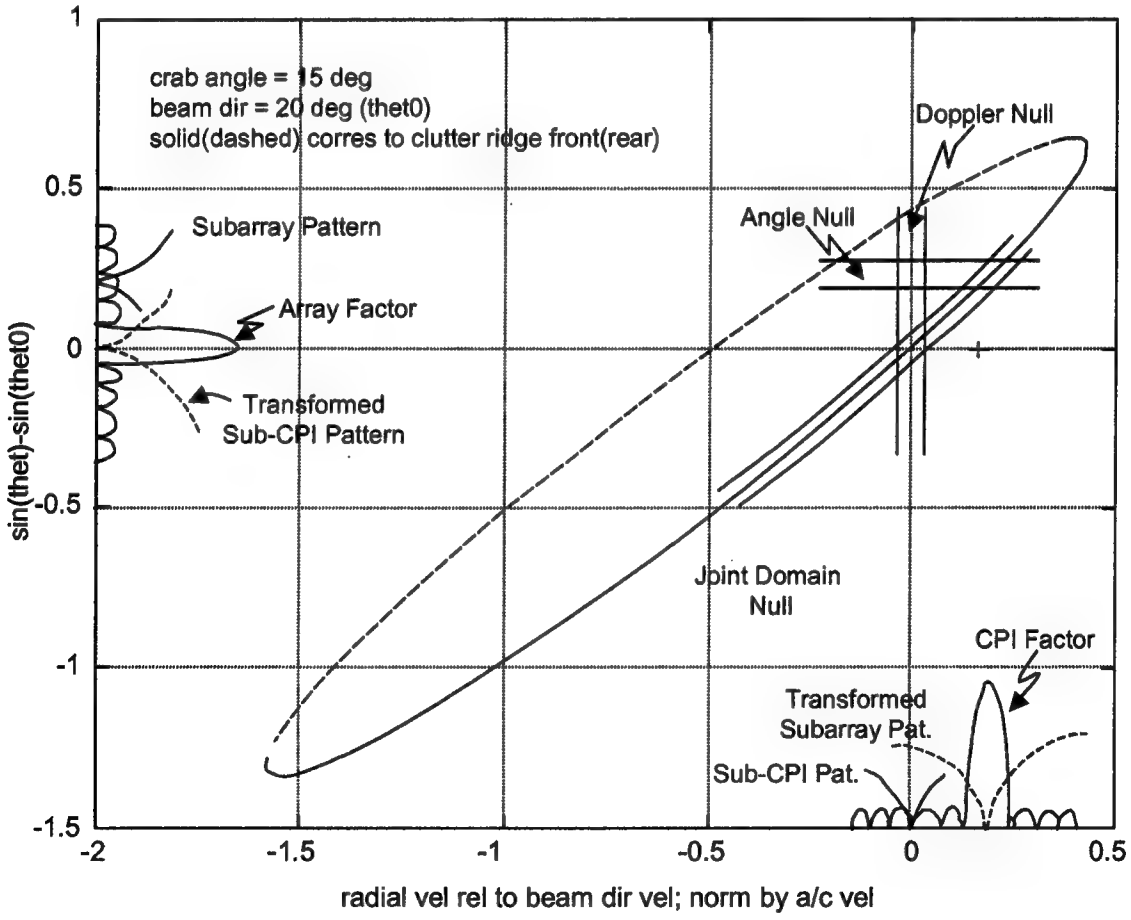

Figure 2-1: Normalized Angle/Doppler Diagram

In principle, the subarray and sub-CPI weights can be jointly determined to null the clutter ridge as suggested by the ribbon that follows the ridge. Such "joint domain subarraying" requires the application of $\sim n_a n_d$ subarrays where n_a is the number of array elements (or columns) and n_d is the number of pulses in the CPI as suggested by the two dimensional overlapped subarrays of Figure 2-2. The aforementioned "factored" approach requires only $\sim n_a + n_d$ sub arrays/sub-CPIs. The factored approach is pursued further here. The joint approach has been studied by others [2].

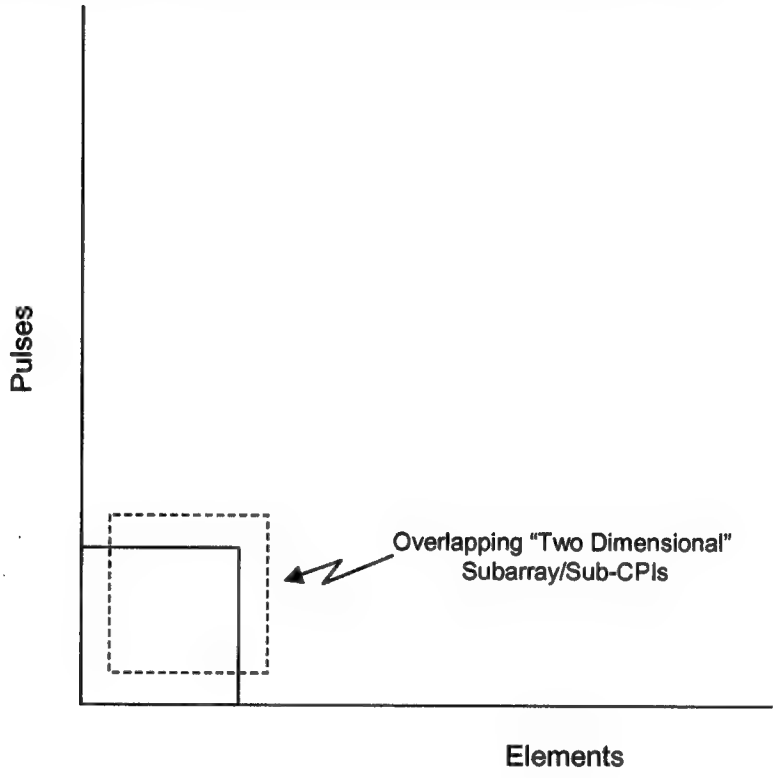

Figure 2-2: Joint Domain Subarray/Sub-CPI

The array factor and CPI factor, as indicated above, can be determined either deterministically (e.g., Displaced Phase Center Antenna) or adaptively (STAP). If moving interference is potentially strong in the Doppler cell and range cell under test, a small DOF STAP method preceded by angle or Doppler notching is preferred. If strong moving interference is not likely, a large DOF method is preferred. The detailed decision process and choice of deterministic or STAP methods is described in Rule 3 in Reference 1.

An iterative procedure for optimizing the subarray/sub-CPI sizes and array factor/CPI factor sidelobe weights is described as Rule 1 and Rule 2 of Reference 1. These parameters are determined by constrained optimization. The objective is to suppress mainlobe clutter while maintaining a minimum signal to noise ratio. It often is desirable to suppress clutter well below noise (by 10 or 15 dB) because of the large uncertainty in clutter statistics. The greater the clutter suppression, the easier it is to meet specified detection and false alarm probabilities. The signal to noise constraint is enforced by requiring that the "processing margin," defined as the allowable signal to interference plus noise degradation resulting form interference suppression processing, be met. If the margin cannot be met, the filter processor reports a degraded probability of detection.

2.3 Procedure

An overview of the constrained optimization procedure is described here. Detailed relations and discussions are given in Rules 1 and 2 of Reference 1.

The procedure can be divided into eight steps. These are defined below.

Step 1: Choose transmit, receive, and Doppler sidelobe levels consistent with required antenna and filter resolutions. The array factor and CPI factor weightings will correspond to these sidelobe levels. [If adaptivity (STAP) is to be applied to determine these factors, the weighting of the space/time steering vector will correspond to these sidelobe levels.]

Step 2: Determine the beam broadening factors (β_a, β_d) corresponding to the angle/Doppler sidelobe levels ($\beta_a = 1$ for uniform weighted receive aperture and $\beta_d = 1$ for uniform weighted Doppler filter).

Step 3: Determine the antenna beamwidth (v_w) in radial velocity (normalized Doppler) space according to

$$v_w = dv_r d\psi\big|_{\psi=0} \beta_a \lambda / D$$

and the radial velocity filter beamwidth (ψw) in angle space according to

$$\psi_w = d\psi / dv_r\big|_{vr=vt} \beta_d \lambda / (2T_{CPI})$$

where v_r = radial velocity coordinate, v_t = the radial velocity of the test Doppler cell, ψ = sine angle coordinate normalized to the beam direction, D = receive aperture extent horizontal dimension, T_{CPI} = CPI duration, and λ = wavelength.

Step 4. Determine the number of subarray elements (n_{rs}) and number of sub-CPI elements (n_{ds}) from normalized binomial distribution patterns. Require that respective null widths be v_w and ψ_w such that within these widths the null depths not exceed the respective CPI factor and array factor sidelobe levels.

Step 5. Determine the processing loss, f_1, according to

$$f_1 = \left(\eta_{eff} G_{rs}(0) G_{ds}(v_t)\right)^{-1}$$

where η_{eff} = product of antenna and Doppler filter "aperture" efficiencies ("weighting losses"), $G_{rs}(\psi)$ = subarray scan loss, and $G_{ds}(v_t)$ = sub-CPI scan loss.

Step 6. If $f_1 \le r$, where r = processing margin, terminate the algorithm. If not, continue. The processing margin is the ratio of the estimated SNR in the absence of clutter and with uniform

antenna/Doppler weightings (maximum quiescent SNR) to the SNR required to achieve a desired probability of detection and probability of false alarm.

Step 7. A minimum amount of mainlobe clutter is allowed to pass. If $G_{rs}(0) < G_{ds}(v_f)$, n_{rs} is reduced by 1. Otherwise, n_{ds} is reduced by 1.

Step 8. Return to Step 5.

An appealing variant of this algorithm would be to modify Steps 2, 3. 4, 6, 7, and 8 such that $n_{rs} = 1$ and $n_{ds} = 1$ initially and are incremented while monitoring an estimate of "signal to clutter ratio improvement (SCRI)" along with f_l. (A means of estimating SCRI is described in the next section by means of example.) The values of n_{rs} and n_{ds} that maximize SCRI within the Step 6 constraint on f_l are accepted as solutions. This variant is not included in the rules of Reference 1.

2.4 Example

An example of the above subarray/sub-CPI design algorithm is given here. Consider the following monostatic radar parameter values.

- Crab angle = 15 degrees
- Beam direction (θ_0) = 20 degrees
- Platform velocity = 150 m/s
- Beam direction velocity = 86.036 m/s
- Target radial velocity w/to beam direction velocity = 25 m/s
- Transit Taylor sidelobe level = 25 dB
- Receive Taylor sidelobe level = 25 dB
- Array length = 18.2λ
- Number of elements (columns) = 36
- Doppler Taylor sidelobe level = 60 dB
- Frequency = 3300 MHz
- Number of pulses in CPI = 128
- PRF = 6 KHz

The relevant angle/Doppler diagram is shown in Figure 2-3. Doppler and two-way antenna clutter response functions are also shown in Figure 2-3. "Clutter response function" refers, here, to the relevant filter output corresponding to clutter distributed uniformly along the clutter ridge. The subarray, sub-CPI, array factor, and CPI factor clutter response functions for 3-element subarrays and 4-pulse sub-CPIs (n_{rs} = 3 and n_{ds} = 4) are shown in Figure 2-4. These subarray/sub-CPI sizes were estimated, using the methods discussed above, to suppress mainlobe clutter to the sidelobe level. Clearly this is the case as is evident from Figure 2-4 by noting where the sub-CPI and array factor patterns cross and where the subarray and CPI factor patterns cross.

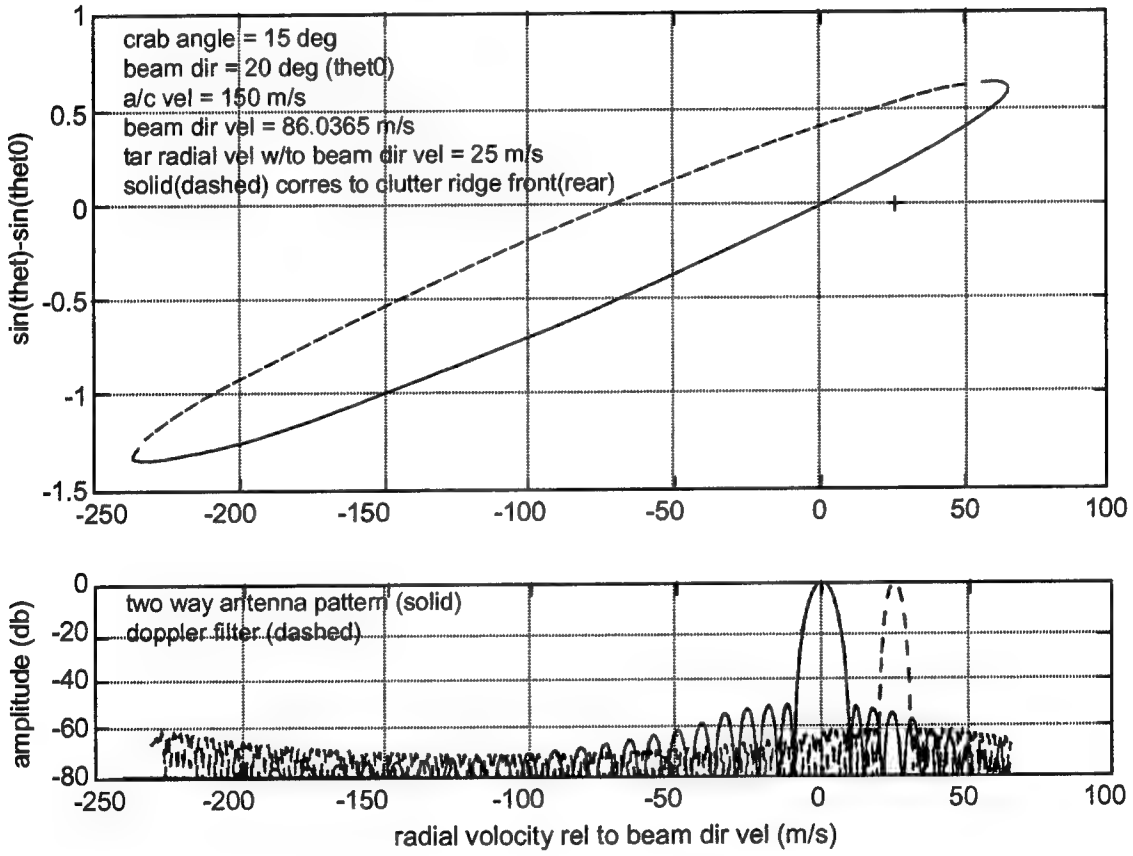

Figure 2-3: Angle/Doppler Diagram (Top); Clutter Response Functions (Bottom)

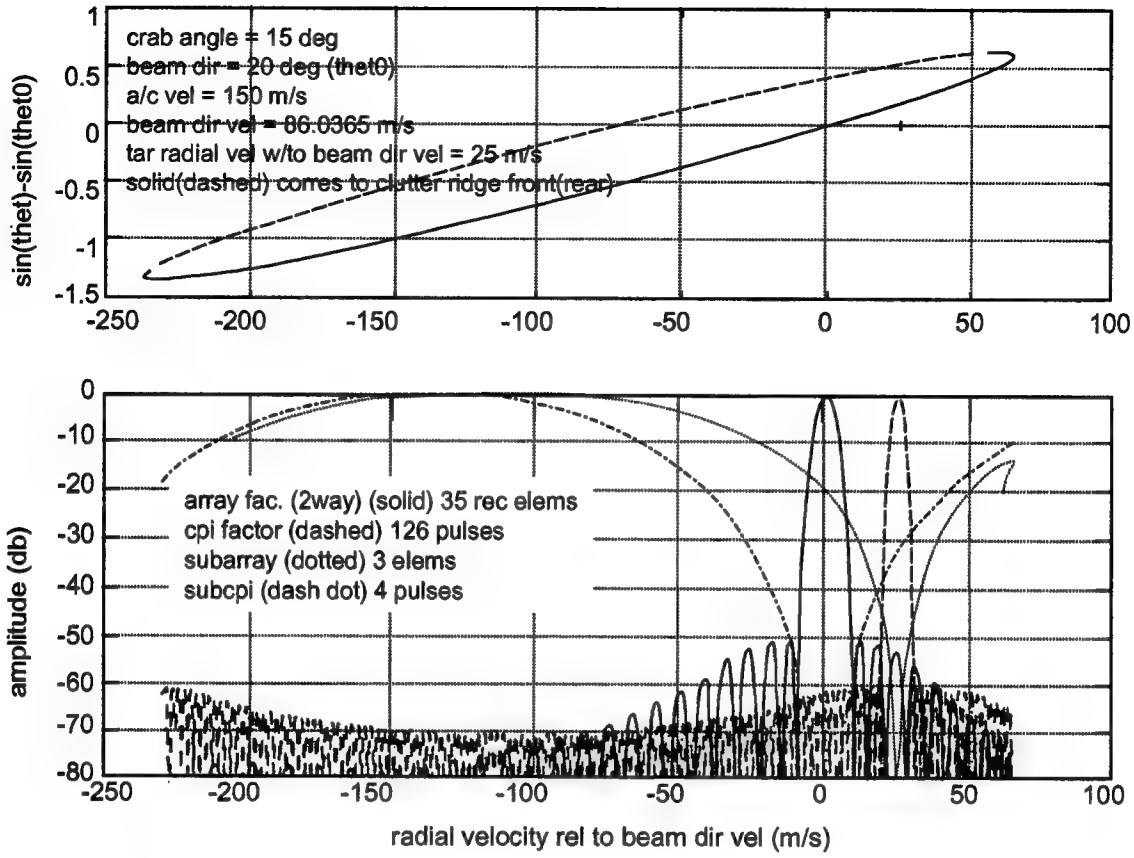

Figure 2-4: Angle/Doppler Diagram (Top), Sub CPI, Array Factor, and CPI Factor Clutter Response Functions (Bottom) for 3-Element Subarrays and 4-Pulse Sub-CPIs

The resulting two-way antenna pattern (product of transmit pattern, receive array factor, and receive subarray pattern) and Doppler filter function (product of CPI factor and sub-CPI pattern) are shown in Figure 2-5. These are the angle/Doppler (or "space/time") ground clutter response functions corresponding to 3 element subarraying and 4 pulse sub-CPIing. The sidelobe levels are clearly affected by the subarray and sub-CPI patterns. The space-time sidelobe clutter response function is the product of the two-way antenna pattern and Doppler filter function and is plotted in Figure 2-6 normalized to the mainlobe space/time clutter response. The peak sidelobe level thus is 92.4 dB below the mainlobe level. (This relative space/time filter sidelobe level is denoted, here, by $f_p = 92.4$ dB.) This value is a measure of clutter suppression associated with subarraying/sub-CPIing. The associated loss (subarray/sub-CPI scan losses plus aperture weighting losses) is computed to be $f_l = 57.5$ dB. A measure of the signal to clutter ratio improvement (SCRI) associated with aperture and Doppler filter weighting and with subarray and sub-CPI nulling, then, is given by SCRI $= f_p - f_l = 34.9$ dB.

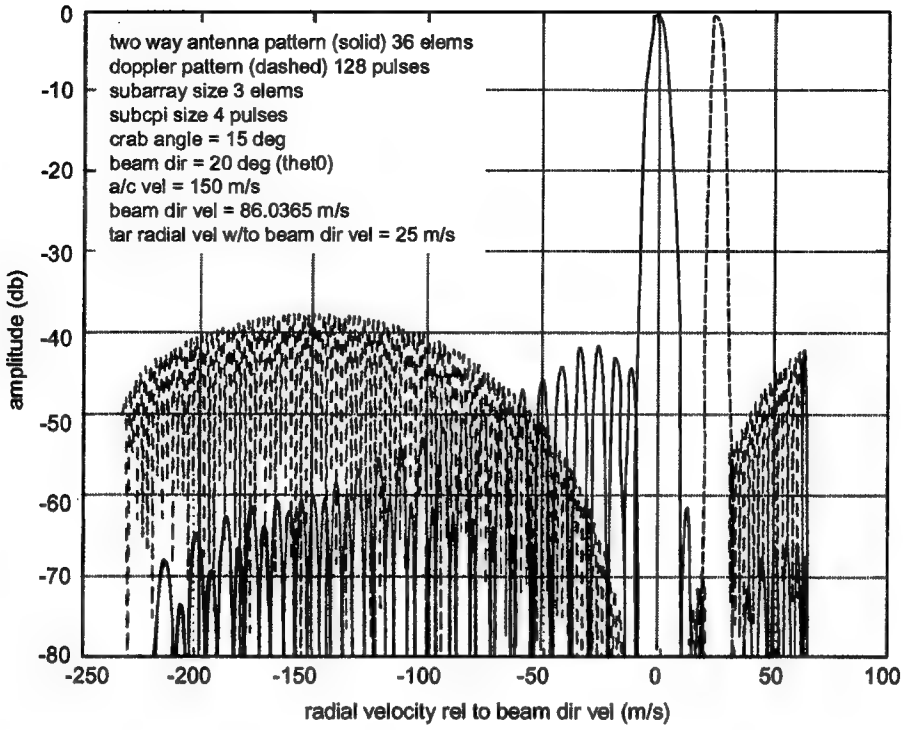

Figure 2-5: Ground Clutter Response Functions for 3-Element Subarrays and 4-Pulse Sub-CPIs

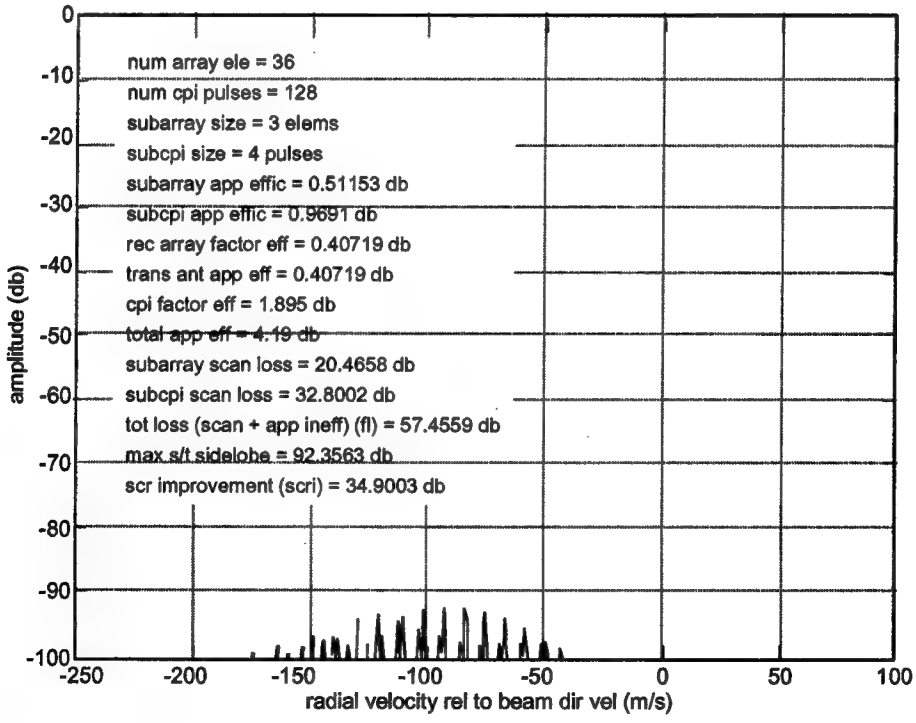

Figure 2-6: Space/Time Sidelobe Clutter Response Normalized to Mainlobe Space/Time Clutter Response for 3-Element Subarrays and 4-Pulse Sub-CPIs

If the processing margin, say, is computed to be 25 dB, f_l = 57.5 dB is unacceptable and some mainlobe clutter is to be allowed. Since the subarray scan loss is $G_{rs}(0)$ = 20.5 dB and the sub-CPI scan loss is $G_{ds}(v_r)$ = 32.8 dB, the largest payoff results from reducing the sub-CPI size by one pulse so that n_{rs} = 3 and n_{ds} = 3. Figures 2-7, 2-8, and 2-9 pertain to this case. The introduction of mainlobe clutter is evident in Figure 2-7 by noting that the sub-CPI and array factor patterns now cross at a level above the sidelobe level. Figure 2-8 shows that the Doppler ground clutter response function sidelobes are still greatly affected by the sub-CPI pattern but not as much as previously (compare with Figure 2-5). Figure 2-9 shows, however, that the peak "sidelobe" clutter now occurs in the mainlobe region. This level, corresponding to f_p = 97.6 dB, suggests greater clutter suppression than before (f_p = 92.4 dB). In fact, since the losses now are reduced to f_l = 46.1 dB, the signal to clutter ratio improvement has actually increased to SCRI = 51.5 dB. (It may be argued that the design procedure should be modified, as discussed briefly in the previous section, to size the subarrays and sub-CPIs so that SCRI is maximized within the constraint that $f_l \leq r$, rather than the current procedure that suppresses only mainlobe clutter under the same constraint. Peak sidelobe clutter may not be as accurately estimated as is mainlobe clutter. Extensive simulations should be conducted to identify the most effective procedure here.)

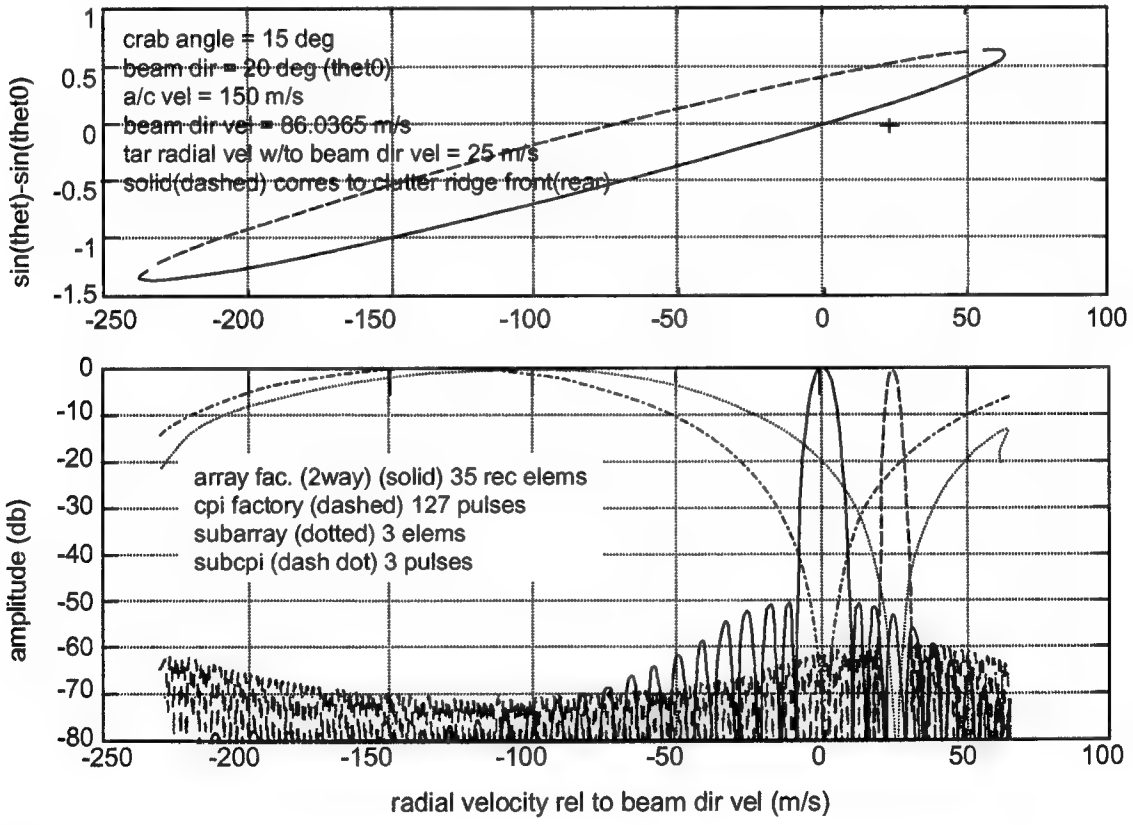

Figure 2-7: Angle/Doppler Diagram (Top); Subarray, Sub-CPI Array Factor, and CPI Factor Clutter Response Functions (Bottom) for 3-Element Subarrays and 3-Pulse Sub-CPIs

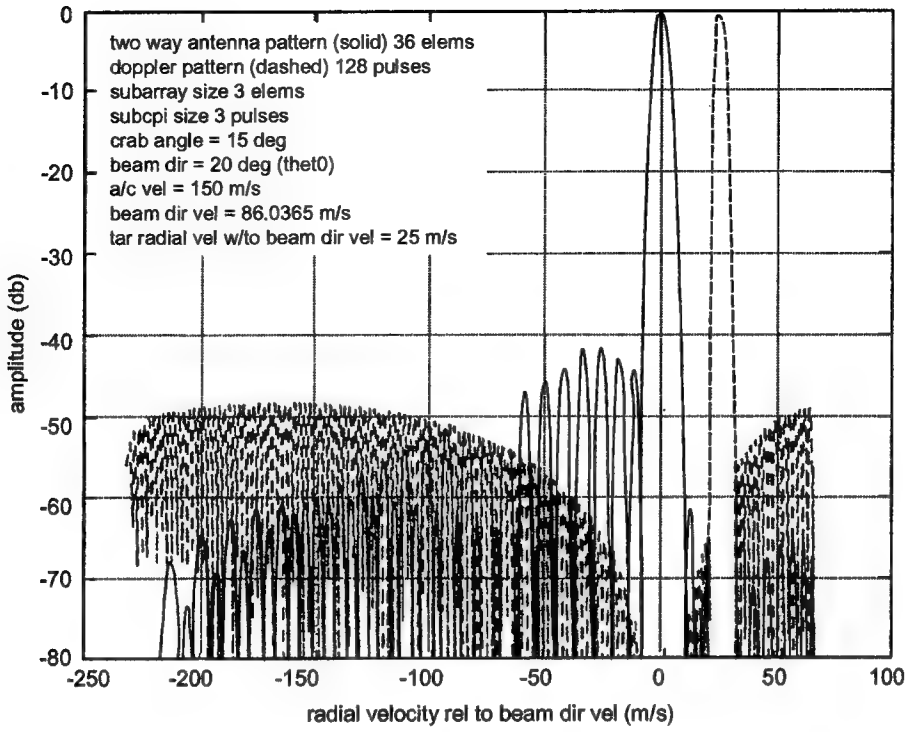

Figure 2-8: Ground Clutter Response Functions for 3-Element Subarrays and 3-Pulse Sub-CPIs

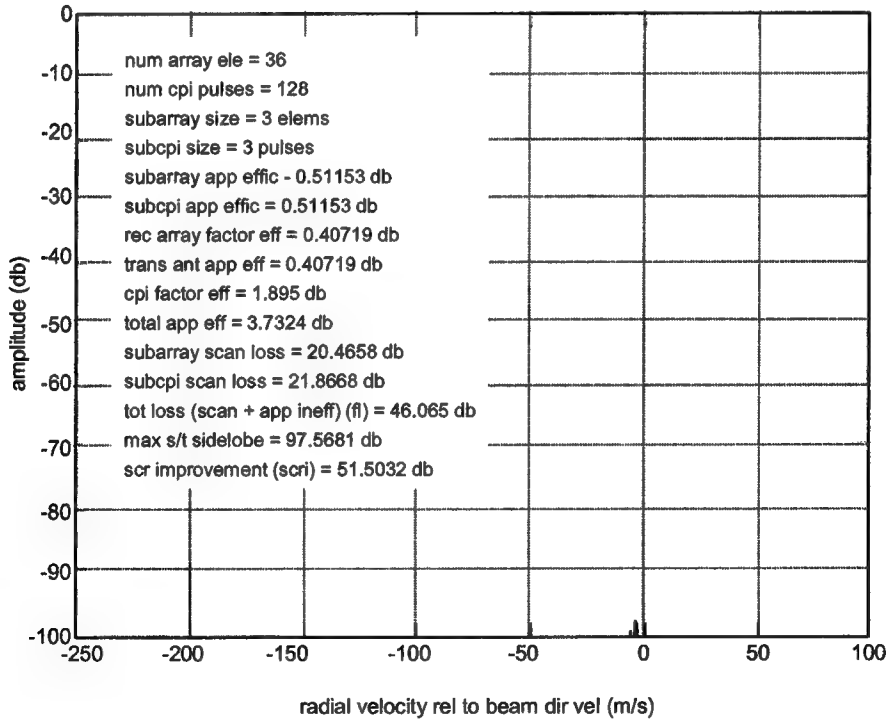

Figure 2-9: Space/Time Sidelobe Clutter Response Normalized to Mainlobe Space/Time Clutter for 3-Element Subarrays and 3-Pulse Sub-CPIs

The losses are still too large. A continuation of the procedure results finally in $n_{rs} = 2$ and $n_{ds} = 2$. Figures 2-10, 2-11, and 2-12 refer to this case. The losses are reduced to 23.9 dB which is within the allowable margin (25 dB). Also, SCRI = 58.2 dB which is an improvement from the $n_{rs} = 3$ and $n_{ds} = 3$ case.

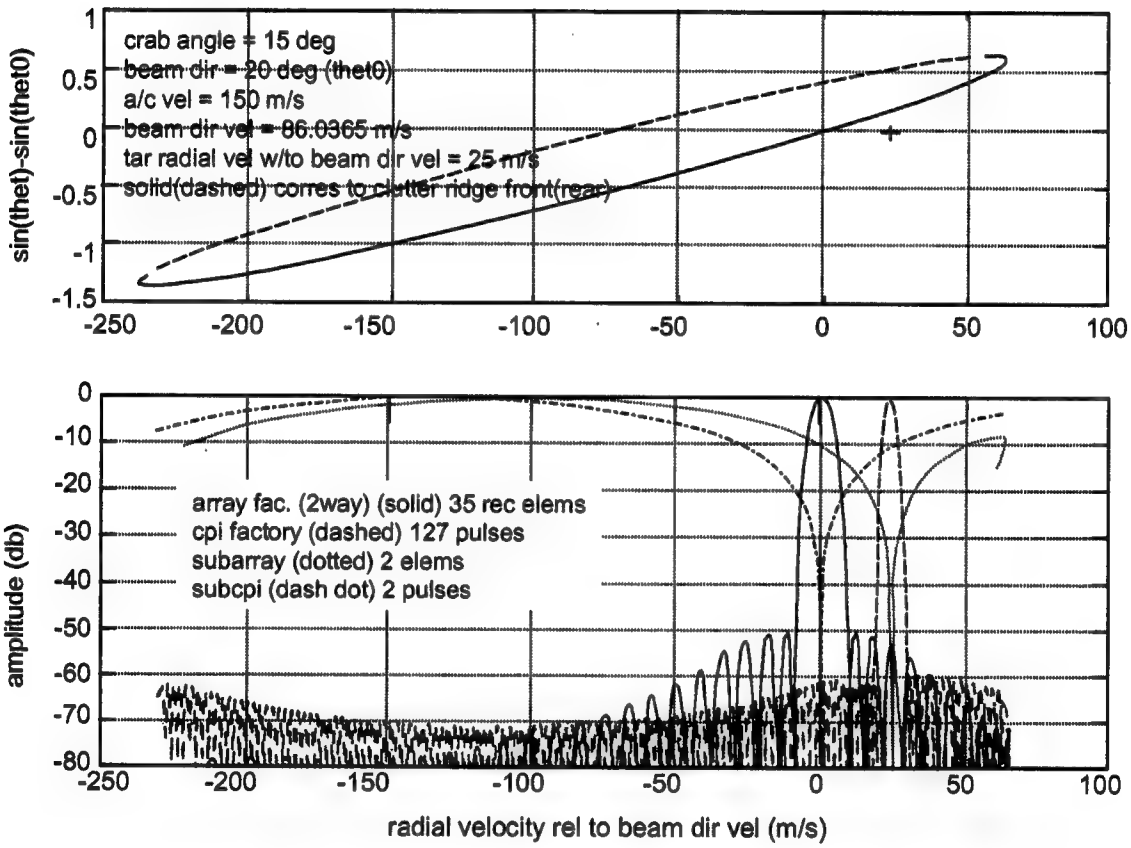

Figure 2-10: Angle/Doppler Diagram (Top); Subarray, Sub-CPI, Array Factor, and CPI Factor Clutter Response Functions (Bottom) for 2-Element Subarrays and 2-Pulse Sub-CPIs

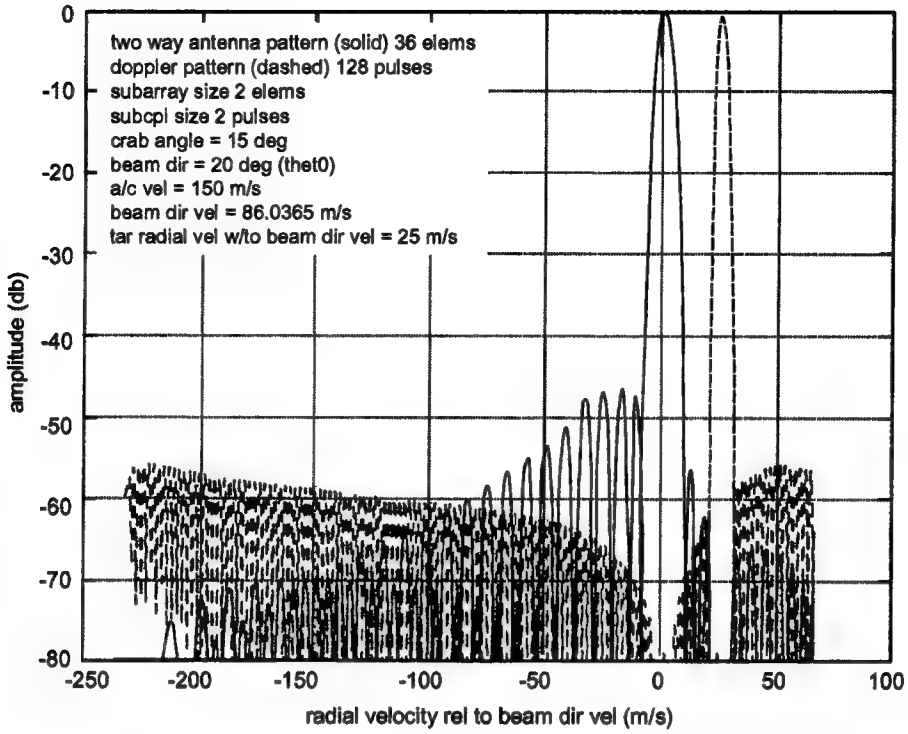

Figure 2-11: Ground Clutter Response Functions for 2-Element Subarrays and 2-Pulse Sub-CPIs

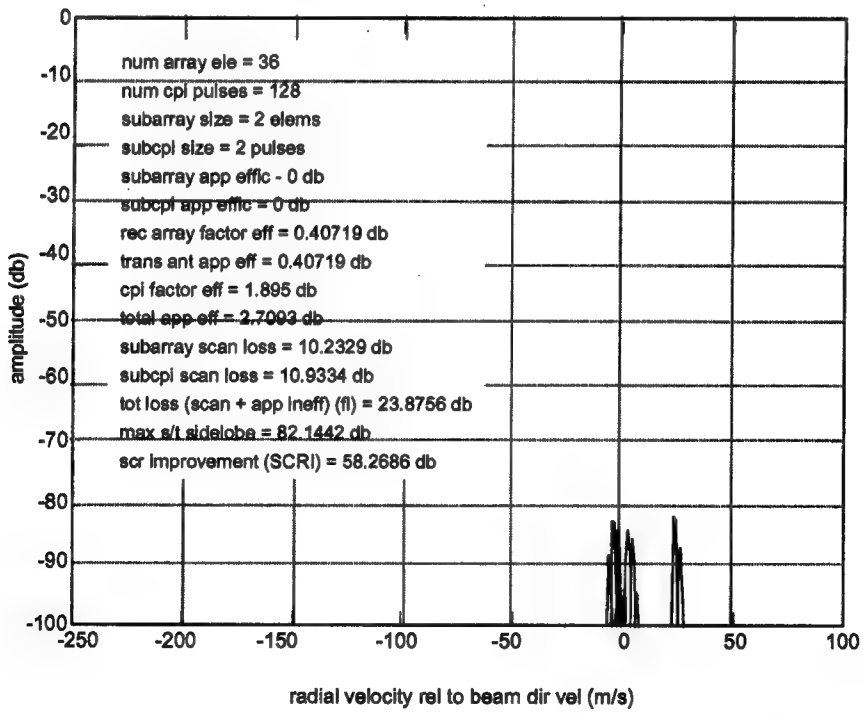

Figure 2-12: Space/Time Sidelobe Clutter Response Normalized to Mainlobe Space/Time Clutter Response for 2-Element Subarrays and 2-Pulse Sub-CPIs

Further reduction in n_{rs} and n_{ds} results in the data shown in Figures 2-13, 2-14, and 2-15 for n_{rs} = 1, n_{ds} = 2 ("two pulse airborne MTI"); Figures 2-16, 2-17 and 2-18 for n_{rs} = 2, n_{ds} = 1 ("subarraying only"); and Figures 2-19, 2-20 and 2-21 for n_{rs} = 1, n_{ds} = 1 ("no subarraying or sub-CPIing"). Coresponding losses are small (13.6, 12.9, and 2.7 dB, respectively), but clutter suppression (SCRI = 40.6, 48.7, and 51.3, respectively) is not as good as in the n_{rs} = 2 and n_{ds} = 2 case. The "subarray patterns" shown dotted in Figures 2-13 and 2-19 are $\cos\theta$ element patterns.

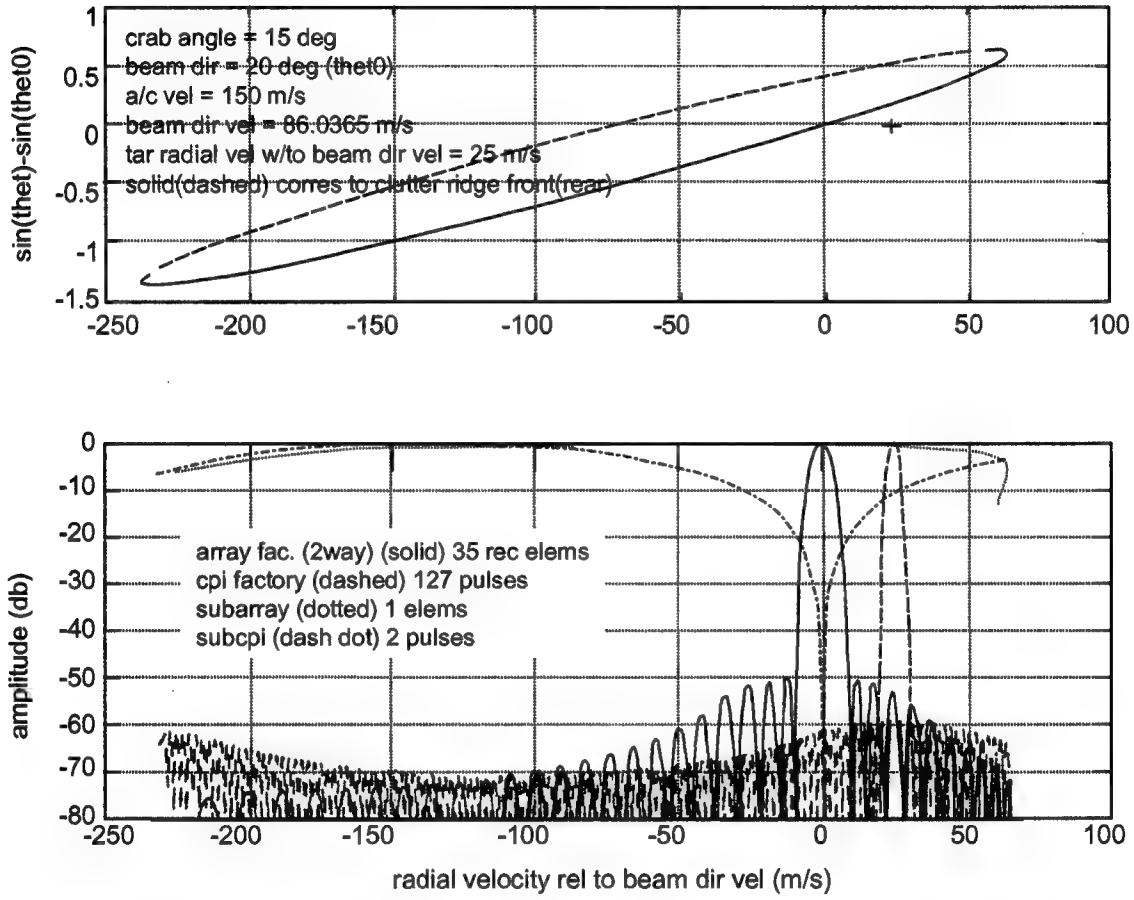

Figure 2-13: Angle/Doppler Diagram (Top); Subarray, Sub-CPI, Array Factor, and CPI Factor Clutter Response Functions (Bottom) for 1-Element Subarrays and 2-Pulse Sub-CPIs ("2-Pulse Airborne MTI")

As a final point, consider the effect of reducing the PRF from 6000 Hz to 4000 Hz. A Doppler ambiguity lobe arises as is evident in Figures 2-22 and 2-23 for n_{rs} = 3 and n_{ds} = 4 case. The subarray pattern clearly does not null the clutter entering the ambiguity lobe. Figure 2-24 shows the corresponding space/time clutter response function. The "sidelobe" clutter peaks at the Doppler ambiguity velocity, as expected. The signal to clutter ratio improvement is only SCRI = 18.0 dB in this case. As indicated in the rule description for subarray/sub-CPI design (Rule 1 in Reference 1), the ambiguity lobe clutter can be nulled as well as the Doppler mainlobe clutter by forming subarrays that

are themselves arrays of subarrays. The combiner weights of one "level" of subarrays are determined by the above procedure to "null" the ambiguity lobe and the weights of the other level of subarrays are determined to null the mainlobe. Ambiguity lobes corresponding to clutter directions exceeding ~70° from broadside, as in the example at hand, could probably be ignored because the antenna element pattern would suppress this clutter.

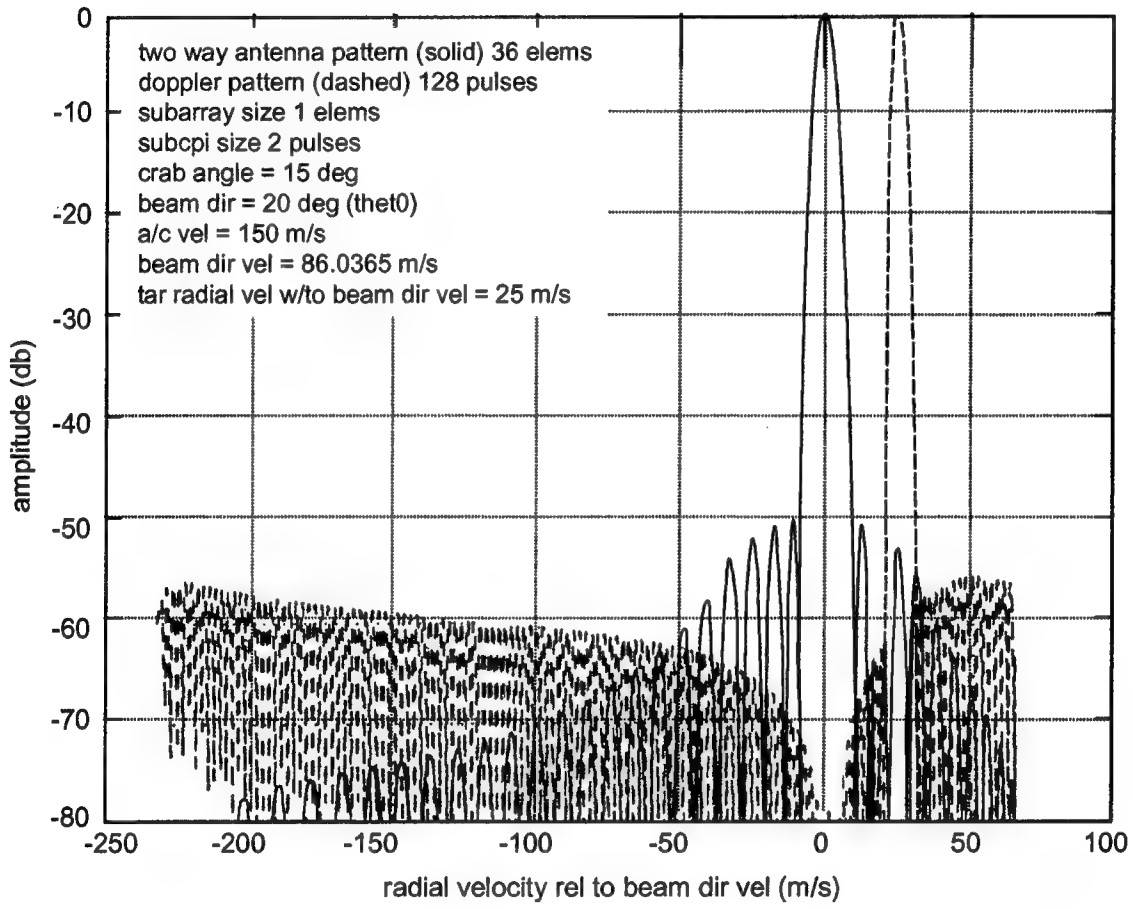

Figure 2-14: Ground Clutter Response Functions for 1-Element Subarrays and 2-Pulse Sub-CPIs ("2-Pulse Airborne MTI")

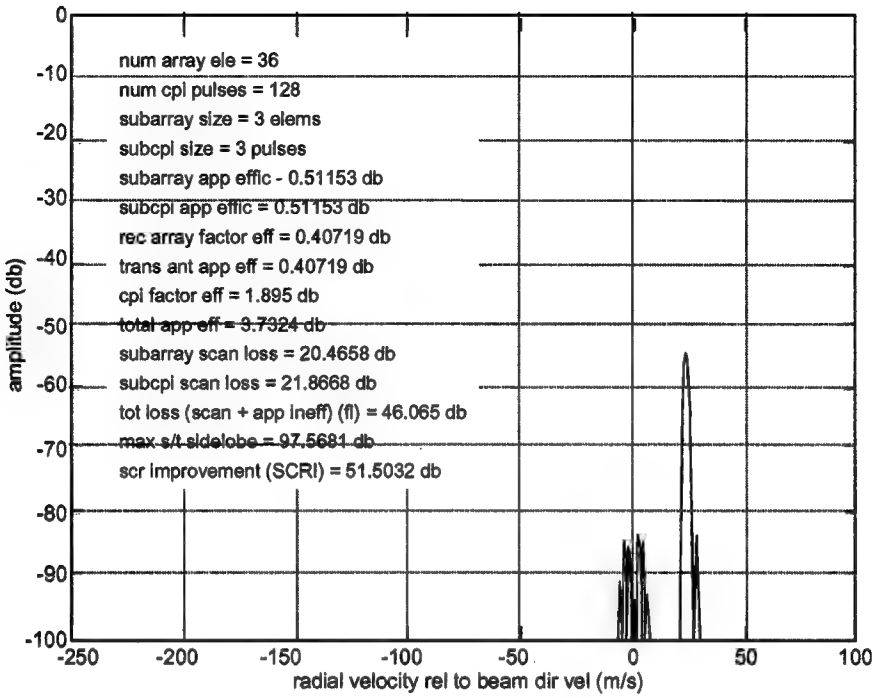

Figure 2-15: Space/Time Sidelobe Clutter Response Normalized to Mainlobe Space/Time Clutter Response for 1-Element Subarrays and 2-Pulse Sub-CPIs ("2-Pulse Airborne MTI")

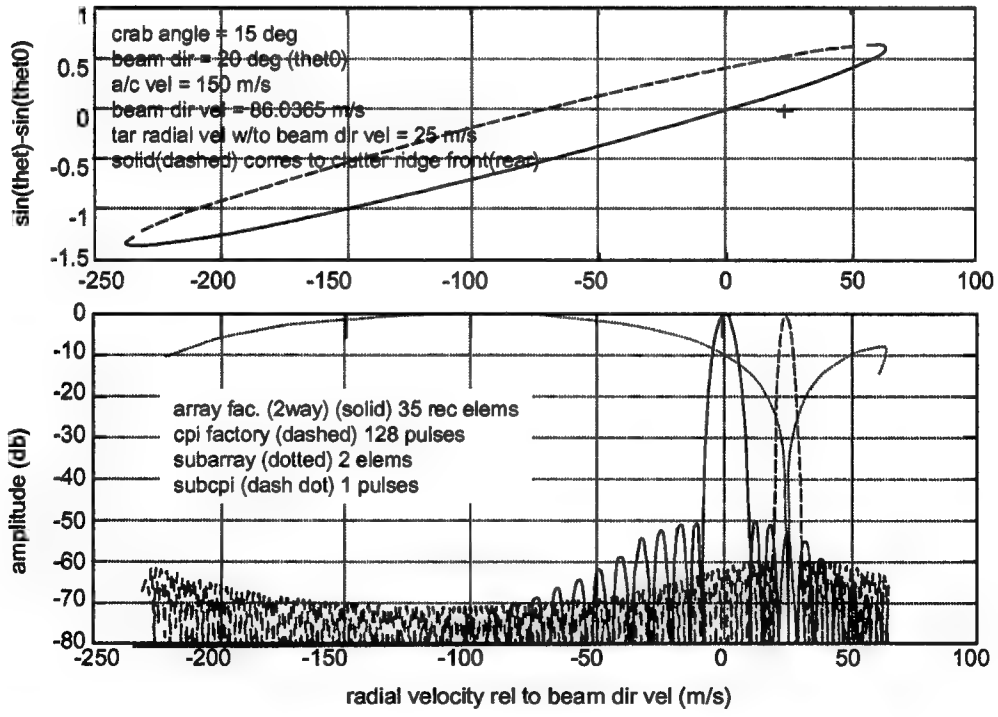

Figure 2-16: Angle/Doppler Diagram (Top); Subarray, Sub-CPI, Array Factor, and CPI Factor Clutter Response Functions (Bottom) for 2-Element Subarrays and 1-Pulse Sub-CPIs ("subarraying only")

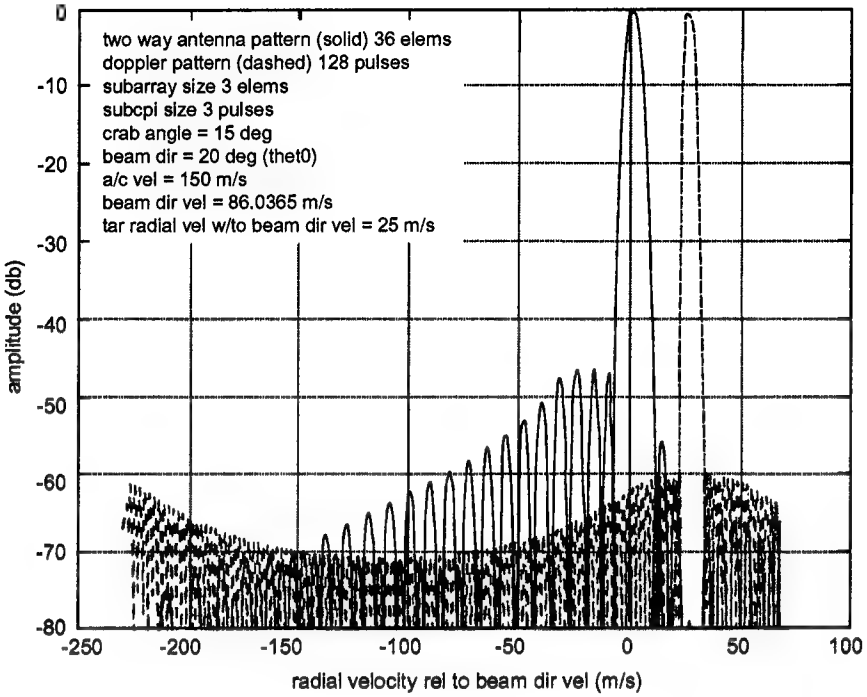

Figure 2-17: Ground Clutter Response Functions for 2-Element Subarrays for 1-Pulse Sub-CPIs ("subarraying only")

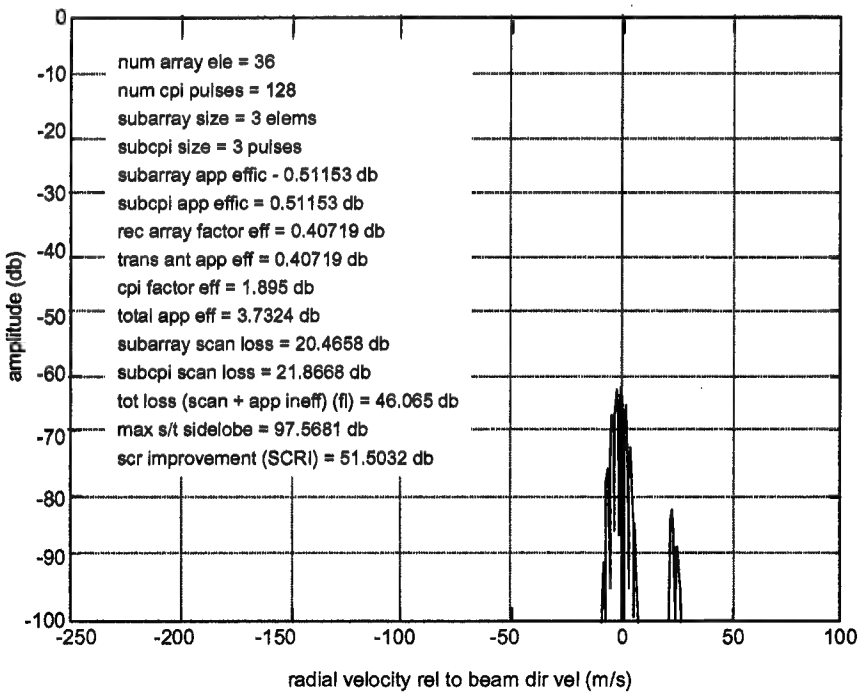

Figure 2-18: Space/Time Sidelobe Clutter Response Normalized to Mainlobe Space/Time Clutter Response for 2-Element Subarrays and 1-Pulse Sub-CPIs ("subarraying only")

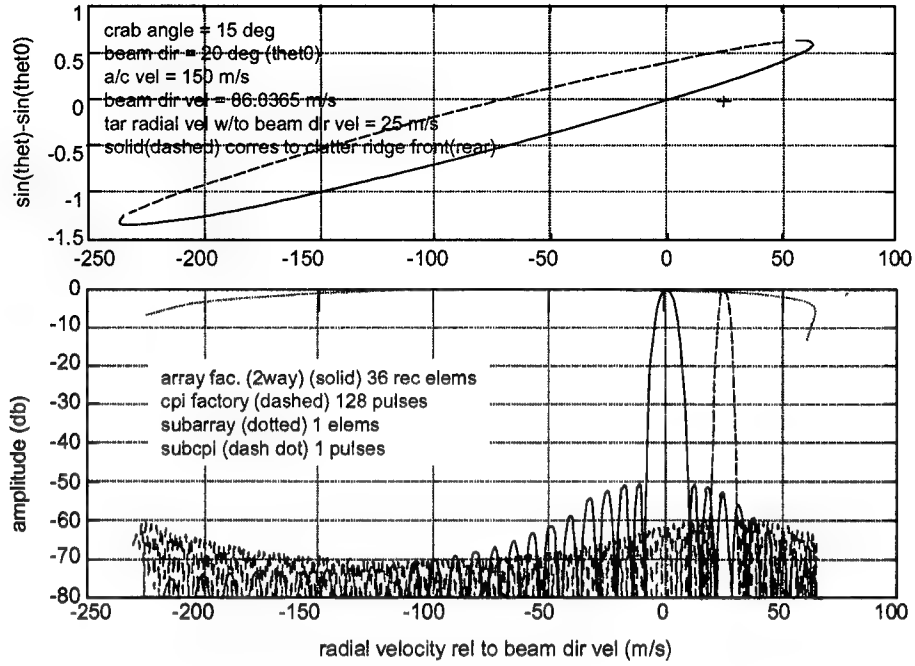

Figure 2-19: Angle/Doppler Diagram (Top); Subarray, Sub-CPI, Array Factor, and CPI Factor Clutter Response Functions (Bottom) for 1-Element Subarrays and 1-Pulse Sub-CPIs ("No Subarraying or Sub-CPIing")

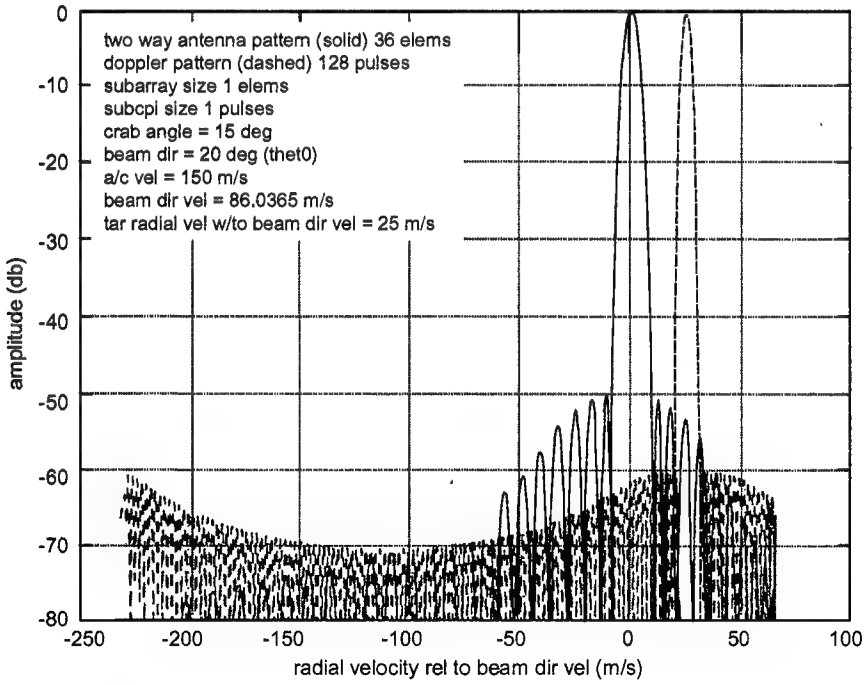

Figure 2-20: Ground Clutter Response Functions for 1-Element Subarrays and 1-Pulse Sub-CPIs ("No Subarraying or Sub-CPIing")

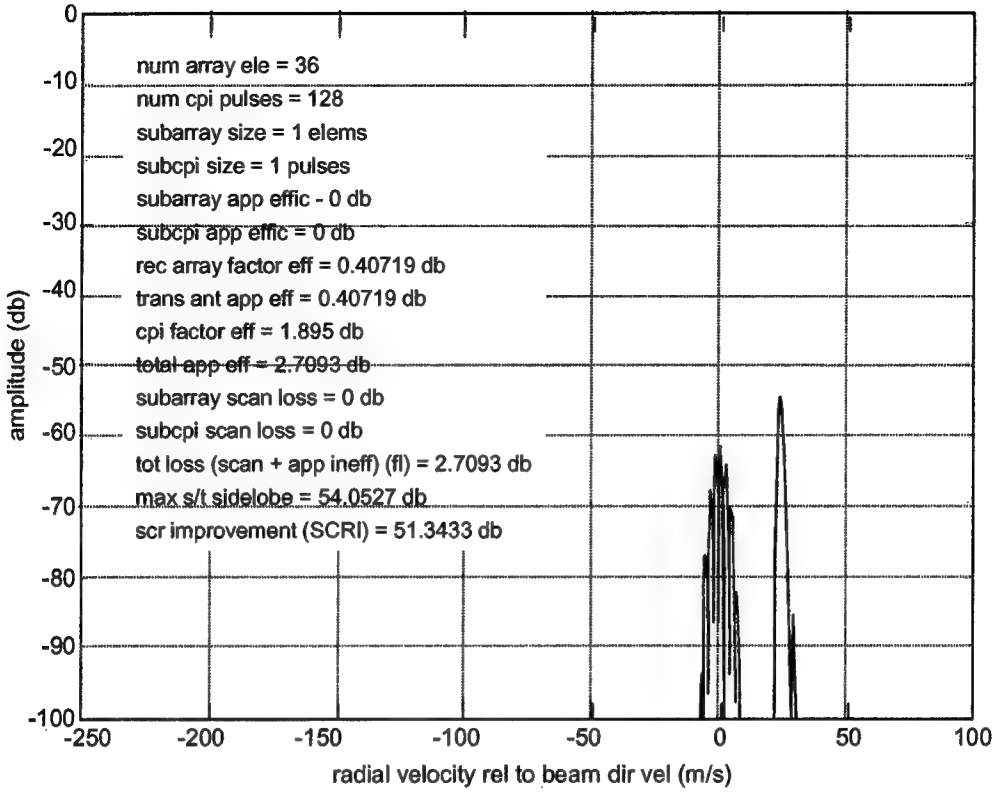

Figure 2-21: Space/Time Clutter Response Normalized to Mainlobe Space/Time Clutter Response for 1-Element Subarrays and 1-Pulse Sub-CPIs ("No Subarraying and No CPIing")

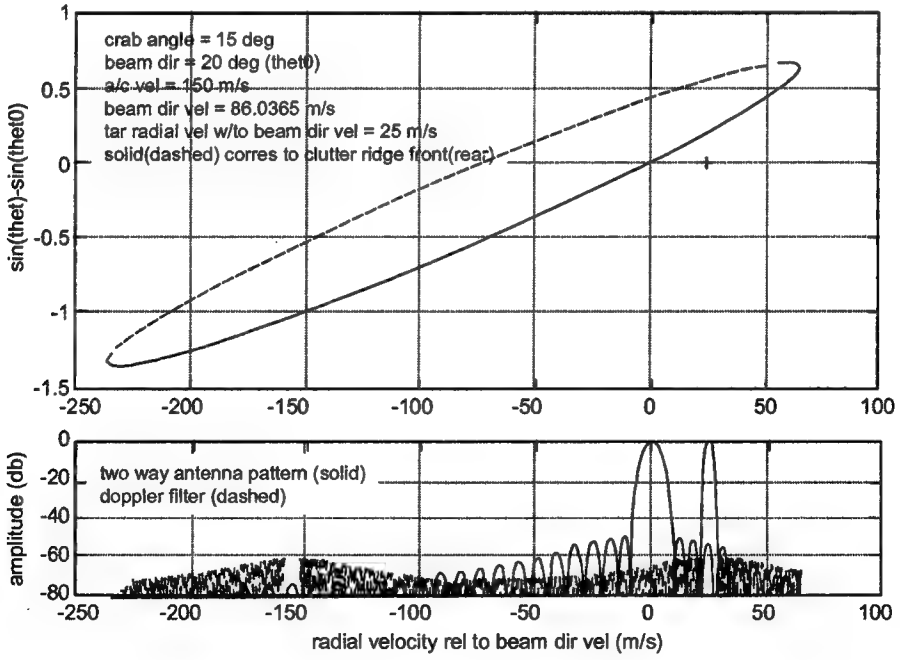

Figure 2-22: Doppler Ambiguous Clutter Response Functions (PRF Reduced to 4 KHz)

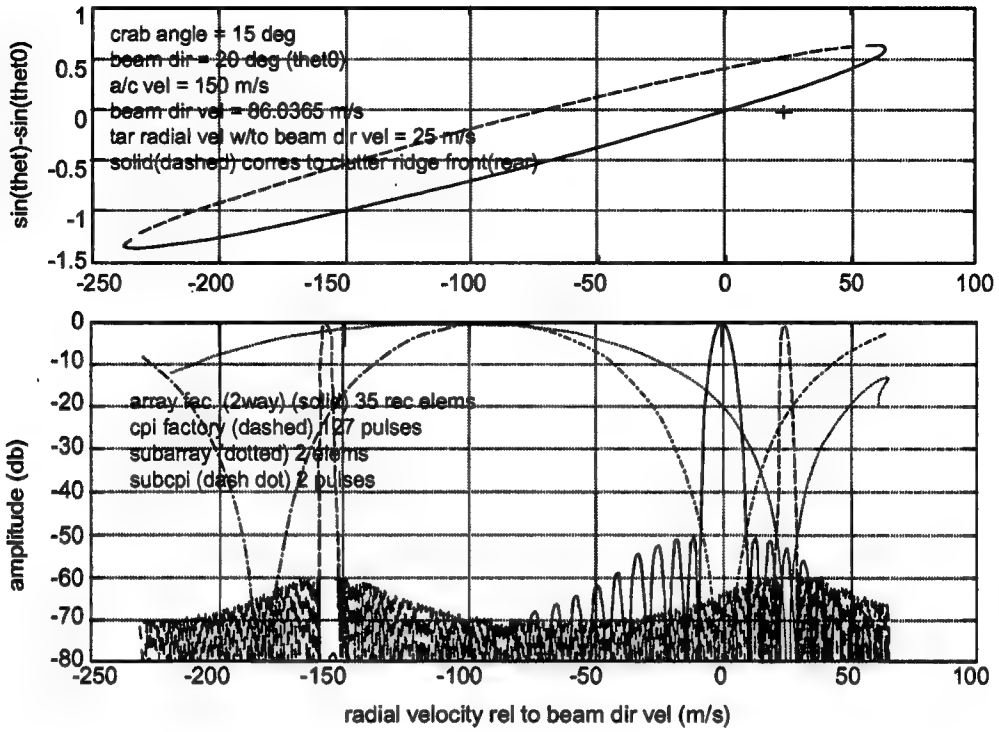

Figure 2-23: Doppler Ambiguous Subarray, Sub-CPI, Array Factor, and CPI Factor Clutter Response Functions (PRF Reduced to 4 KHz)

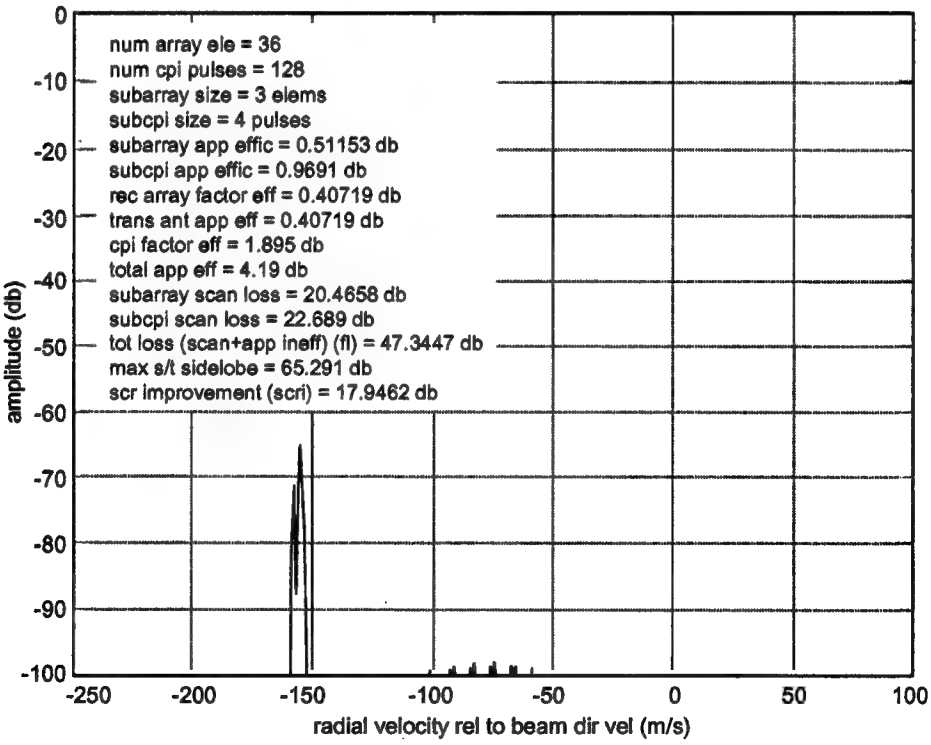

Figure 2-24: Doppler Ambiguous Space/Time Sidelobe Clutter Response Normalized to Mainlobe Clutter Response (PRF Reduced to 4 KHz)

Section 2.0 References

1. "Radar Filtering Rulebook," SRC TD 97-1466, Syracuse Research Corporation, Syracuse, NY, 31 October 1997.

2. J. McClellan, et. Al., "Direct Clutter Cancellation for STAP," *Proceedings of the ASAP Working 13-15 March 1996 (at MIT Lincoln Laboratory)*, P. A. Netishen, ed., pp 97-123, 29 April 1996.

Section 3.0
Array Notching and Spatial Only Adaptivity

Syracuse Research Corporation
February 17, 1998

3.1 Introduction

Space Time Adaptive Processing (STAP) has been found to be largely ineffective in suppressing clutter discretes associated with moving scatterers including airborne and ground traffic. This conclusion is not suprising because STAP is known to be most efficient in suppressing nonmoving interference sources (i.e., clutter ridge sources) and, more importantly, "moving" discretes often are absent or exhibit distorted angle/Doppler profiles in range cells required for covariance matrix estimation.

The effectiveness of STAP in suppressing ridge clutter can be improved by "deterministic prefiltering". Subarray and sub-CPI nulling is an effective method of realizing such prefiltering. This method is described in a separate self contained section of this report and forms the basis of Rule 1 in the Radar Filtering Rulebook [1].

Deterministic "nothing" ("nulling" at the "array factor" level in combination with STAP, on the other hand, has been investigated as a method for suppressing moving discretes and ridge clutter simultaneously. Notching is effective in combination with a small degree of freedom (DOF) STAP method where only a few spatial channels are applied to STAP and the remaining channels are applied to notching. The optimum number, location, and widths of the notches would be determined based upon mapping data identifying highways, etc.; tracking data identifying airborne vehicles; and antenna parameters such as beamwidths and sidelobe levels. The process would draw from waveform parameter data, as well, primarily to identify foldover ranges and Doppler grating lobes. Ideally each range/Doppler cell under test would be processed with a configuration optimum for that cell.

Sidelobe jamming can be suppressed by spatial adaptivity simultaneously with generating the notches for suppression of discretes. Notching and this "spatial only adaptivity" is summarized in the following subsection. An example is described in a concluding subsection. The antenna in the example is a large S-Band planar array (3,456 elements) with 18 coherent receivers. The waveform is range and Doppler ambiguous. Interference from ground clutter, jamming, and highway traffic scattering are included in the example. This antenna/processor is selected because it has the advantage of large "AWACS" size aperture and only a moderate number of receivers. Phase shifters and low sidelobe sum

and difference weights are applied at the element level. Analog combiners are used to divide the array into nine sub-beam subarrays and nine difference-beam subarrays. One receiver is applied to each of the 18 subarray ports. The subarrays are randomly sized to avoid excessively high grating lobes.

3.2 Notching and Spatial-Only Adaptivity

Once potential clutter discretes associated with moving scatterers that reside within the range/Doppler cell under test are identified, appropriate deterministic nulls ("notches") can be synthesized in the antenna patterns. The determination of whether a potential discrete lies within the test cell is a function of the location and velocity of the sources of the discretes. In the case of vehicle traffic, the defining data includes the point where a highway crosses the range cell (or range foldover cell), the orientation of the highway within the cell, and the expected range of vehicle speeds.

Once all potential discretes are identified, two other issues must be addressed. One issue is the priority of discretes. The discretes must be ordered in accordance with potential severity so that the limited spatial channels available for pattern notching can be most effectively utilized. The third issue deals with the width of the notches. These issues are addressed in depth in Section 4 of the "Radar Filtering Rulebook" [1]. Specific relations for building an associated knowledge base processor are given therein, as well.

Consider, first, the issue of identifying a discrete. Access to all airborne traffic data by the radar tracker and, in some instances, by cooperative sensors is assumed. From aircraft range, angle, heading, and speed, a decision clearly can be made as to whether the associated discrete will reside in the range/Doppler cell under test.

In the case of highway traffic, an additional data parameter is required. This parameter is the expected maximum speed of the highway traffic. A highway that crosses a test range cell is a potential source of interference when testing a Doppler cell if the angle to the intersection of the highway and range cell, the maximum expected vehicle speed, and orientation of the highway in the range cell are such that the Doppler of the vehicle scattering falls within the test Doppler cell. (Foldover clutter ridges and foldover range cell discretes must be treated in like manner.) A small angle between highway and range cell may result in the associated highway exciting a distributed type of discrete. This effect would cause the angular extent of the scattering to enlarge and would be characterized by a broadened line in angle/Doppler space. The broadened line, however, also would shorten dramatically (reduced maximum Doppler) and the highway scatterers would appear to nearly reside on the clutter ridge; i.e., appear motionless, or, as is more likely, simply be masked by intrinsic clutter motion scattering.

Another issue is that of notch prioritization. With a limited number of spatial channels available for forming notched antenna patterns, rules for prioritizing the discretes that are candidates for notching must be developed. Potential discretes that can strongly impact the test range/Doppler cell can occur at foldover ranges and angles as well. Priority rules developed and detailed in [1] are based only upon slant range and antenna gain because moving scatterer discretes, as resulting from ground vehicles and

air traffic, are not thought to exhibit the same well defined "grazing angle" dependence as does distributed clutter. Although the intensities of the discretes could be strongly influenced by the orientation of the highway in the range cell, this dependence was not considered in the development of [1]. (The orientation, however, does strongly influence the range of Doppler velocities associated with a highway, and so is a necessary parameter whether a discrete is coincident with a test range/Doppler cell and thus is a candidate for notching as discussed above.) The moving discretes are likely to behave as point scatterers with a R^{-4} range dependence in contrast with distributed clutter that is likely to exhibit range dependence closer to R^{-2} or R^{-3}.

Consider now, the issue of determining notch width. The choice of width of an antenna pattern notch for suppressing highway traffic discretes is governed primarily by the angle and the depth at which a null can be formed. The null depth, typically given in "dB below the quiescent sidelobe level" is limited, in turn, by antenna errors. In some cases, a notch width larger than that required to suppress a discrete in the vicinity of the test cell may be desired so that the corresponding highway is notched as well in neighboring range cells. These neighboring cells then are likely to function better as STAP reference cells.

A rough relation between number of spatial channels devoted to forming a notch, notch depth, notch angular location from broadside in the cardinal horizontal plane, antenna aperture extent in the horizontal plane, wavelength, and notch width has been derived [1].

Figure 3-1 shows an associated antenna/filter architecture. The notching and spatial only adaptivity is carried out simultaneously, i.e.; one set of weights is determined that simultaneously nulls jamming and "notches" clutter discretes. Doppler filtering precedes the STAP processor because it has been shown that small DOF STAP methods are most effective when preceded by all available deterministic filtering including temporal (Doppler) and spatial (low sidelobes, notching). (This conclusion is explored in the self contained section on STAP under separate cover.) In Figure 3-1, the R matrices are the appropriate covariance matrices: the jamming covariance matrix is denoted R_a, the notching covariance matrix is denoted R_d. The matrix R_d can be determined by creating unit power jamming that fills the notched angular regions [2]. The coefficient β then is the desired level of created interference power with respect to noise power. The appropriate level can be estimated from the curves of Figure 3-2 for .5 and 1.0 degree wide notches in sum and difference patterns. (This design data was not included in the Rulebook[1].) Here, the notches are assumed to be specified in symmetric pairs about boresight in order to help preserve the symmetry of the sum and difference patterns and minimize monopulse angle estimation inaccuracy. The coefficient α reflects diagonal loading the amount of which is discussed in Section 3 of [1].

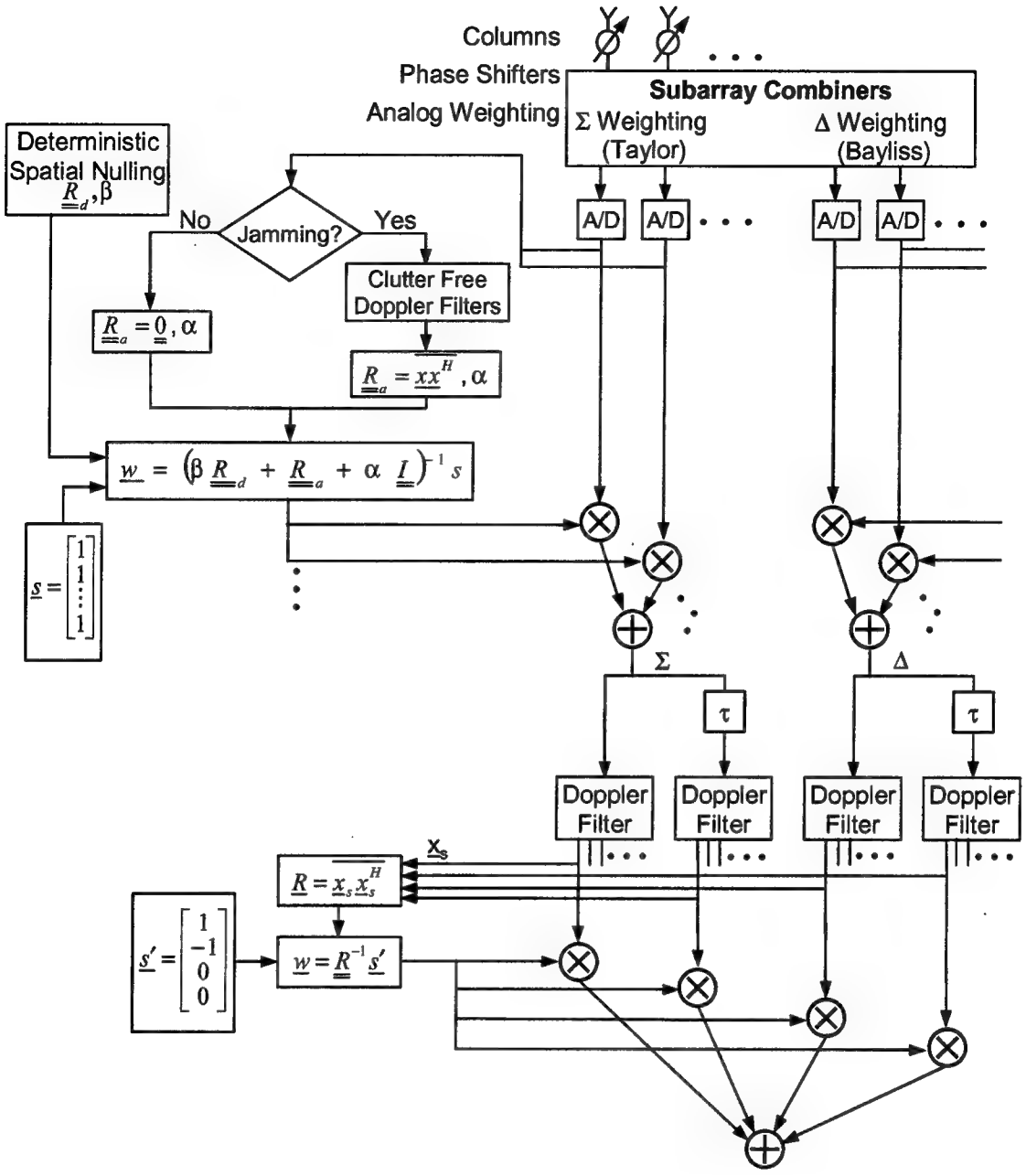

Figure 3-1: Small Degree of Freedom STAP Filter Architecture

Analog weighted beam forming is indicated in Figure 3-1. Alternatively, the subarrays can be formed digitally to exhibit subarray patterns with nulls positioned to suppress ground clutter that resides along those parts of the clutter ridge that intersect the Doppler filter main lobe and ambiguity lobes. The design considerations are described in aforementioned separate self contained section of this report (entitled "subarray/Sub-CPI Nullng"). Although not shown in Figure 3-1, the deterministic nulling/spatial only adaptivity part of the architecture is assumed to be duplicated for application to the difference pattern.

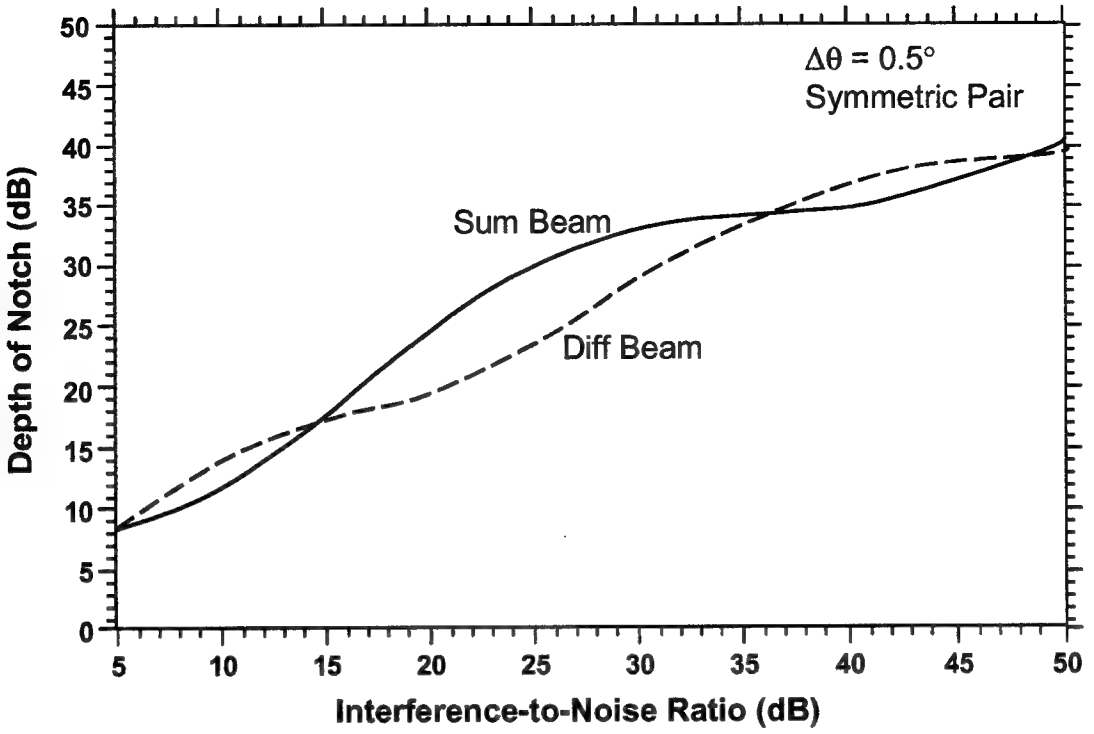

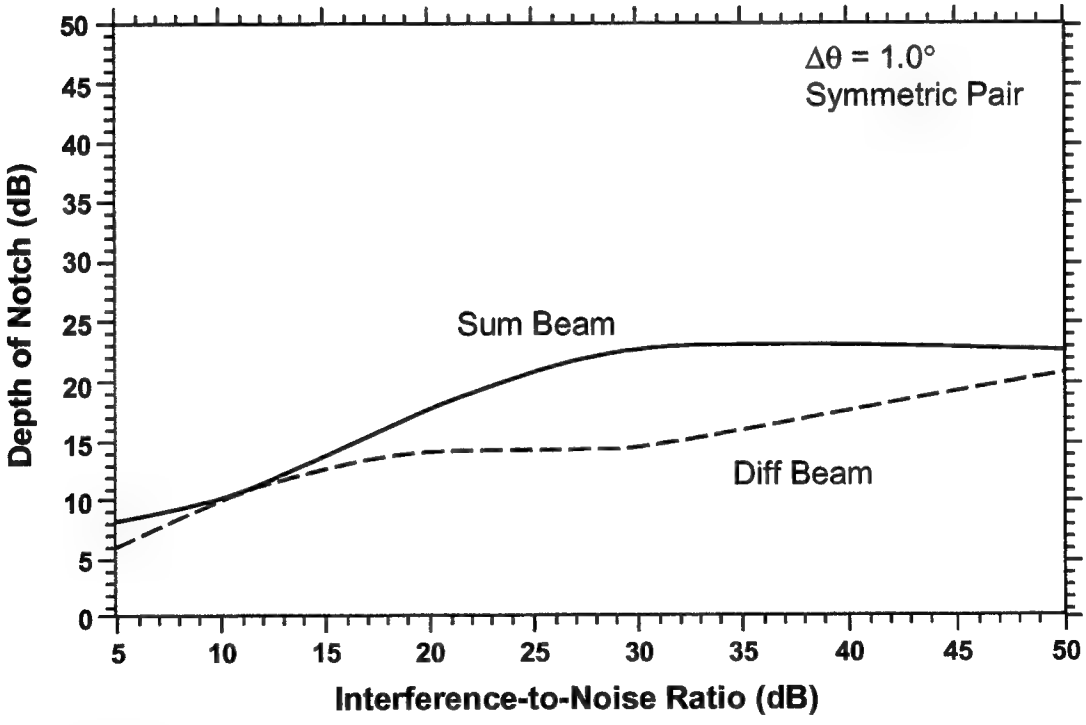

Figure 3-2: Deterministic Notching (Pattern Synthesis) Design Curves

Figure 3-3 shows an alternative large DOF STAP configuration. Here, subarray channels are combined with the sum and difference channels forming a "joint beam and subarrays," two pulse, post Doppler, adaptive DPCA STAP processor (referred to as "SLC Post Doppler ADPCA" in the aforementioned separate self contained section of this report entitled "Space/Time Adaptive Processing"). The large DOF STAP configuration would be favored when testing range/Doppler cells devoid of discretes.

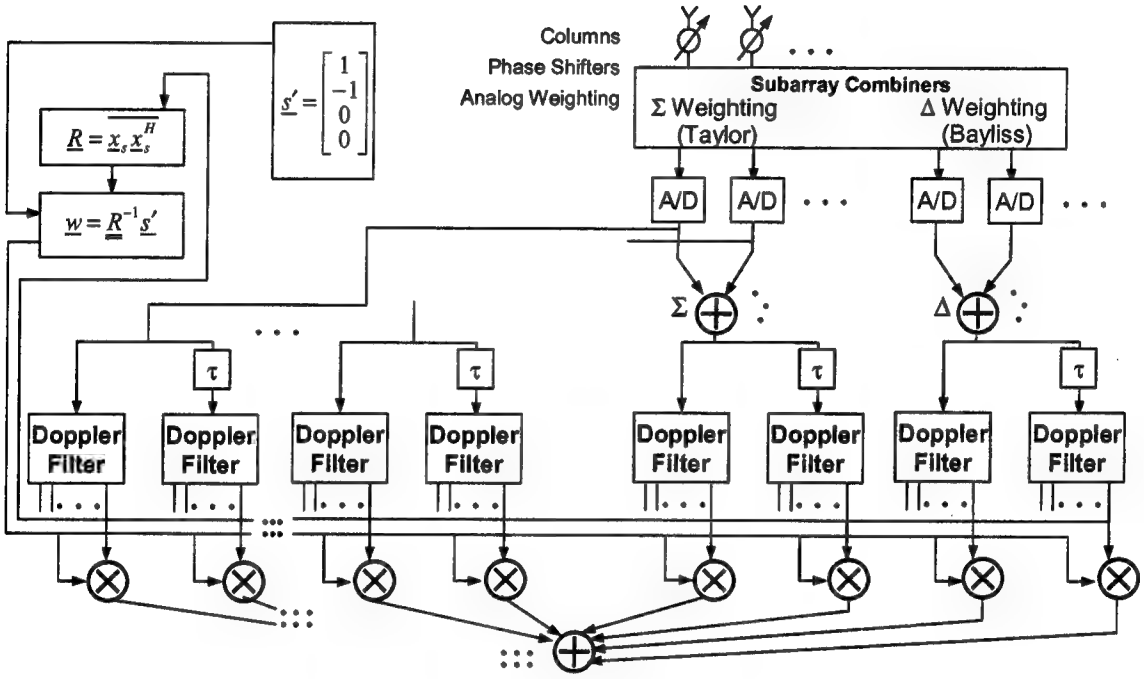

Figure 3-3: Large Degree of Freedom STAP Filter Architecture

3.3 Example

An example that illustrates the benefit of notching is given here. In this example, notching is applied to suppressing highway traffic clutter, spatial only adaptivity is applied to suppressing jamming, and the small DOF STAP method of Figure 3-1, "sum and difference beam post Doppler adaptive DPCA," is applied to suppressing ridge clutter. The Figure 3-2 configuration is applied to the same scenario for comparison.

The antenna configuration is a large S-Band rectangular array with 16 rows and 216 columns of elements. The array is fully populated with phase shifters to retain low sidelobes with scan over a wide field of view (FOV) in azimuth and limited FOV in elevation. Three manifolds provide uniform illumination for transmit; 35 dB Taylor azimuth and 35 dB Taylor elevation for the sum beam; and 35 dB Bayliss azimuth and 35 dB Taylor elevation for the difference beam. Each receive beam manifold is divided along the azimuth axis into nine submanifolds that feed contiguous subarrays (Figure 3-4). The

subarray sizes are randomized to avoid excessive grating lobes. (The number of columns in each subarray is shown in Figure 3-5.) A receiver and A/D converter is associated with each submanifold. The nine digital channels for each receive beam provide the flexibility required for the deterministic and adaptive sidelobe nulling procedure. Waveform parameters and aperture data are tabulated below.

Frequency	S-Band
Bandwidth	1 MHz
PRF	2,400 Hz
Altitude	10km
Velocity	150 m/s
Crab	0 degrees
Tilt	5.7 degrees "Down"
CPI	128 Pulses
Azimuth Element Spacing	0.536 λ (implies 120 degrees full FOV in azimuth)
Elevation Element Spacing	0.6 degrees
Aperture Width (Azimuth Dim.)	11.58 m
Aperture Height (Elev Dim.)	0.96 m
Transmit Illumination	Uniform
Receive Illumination Sum	35 dB sidelobe Taylor in az and el
Receive Illumination Diff	35 dB Bayliss in az, 35 dB Taylor in el
Unambiguous Range Interval	62.5 km
Unambiguous Range Rate Interval	120 m/s
Az Transmit 3 dB Beamwidth	0.44 degrees
El Transmit 3 dB Beamwidth	5.29 degrees
Az Receive 3 dB Beamwidth	0.58 degrees
El Receive 3 dB Beamwidth	6.99 degrees

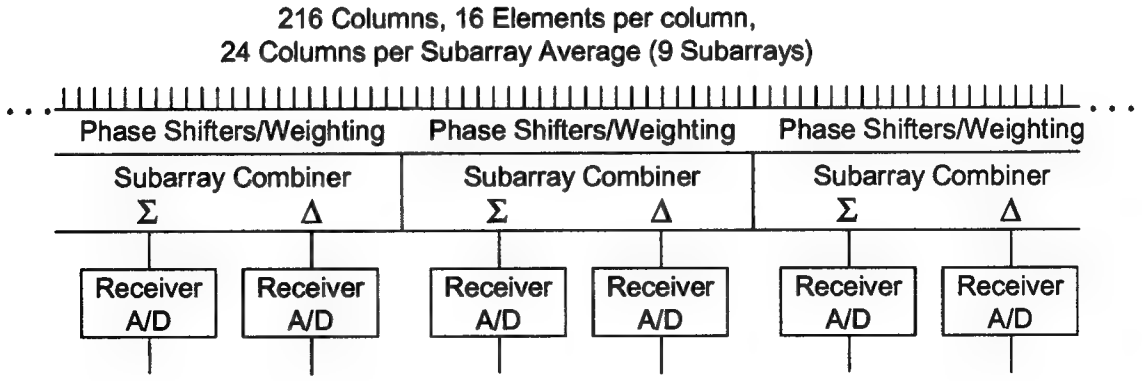

Figure 3-4: Analog Combiner Architecture for Example

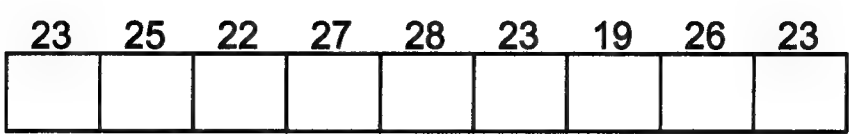

Figure 3-5: Random Sized Subarrays

The geometry is shown in Figure 3-6. The sensor platform is moving at 150 m/s. The target is located at 100 km range, broadside to the antenna and sensor platform, and moving so as to exhibit a 20.2 m/s radial velocity (100 m/s at an angle of 78.3 degrees with respect to normal). A highway crosses the target range circle at 3.4 degrees from broadside. Traffic moves at 30 m/s with respect to ground and the highway makes a 22.4 degree angle with respect to the tangent line of the target range circle at the crossing (67.6 degrees with respect to the radial line). The ground radial velocity (8.9 m/s) plus the vehicle radial velocity results in a discrete at the same range and Doppler as the target. Competing ground clutter (same target Doppler) appears at 7.7 degrees, -41.8 degrees, and 69 degrees from broadside. The latter two angles correspond to locations of Doppler ambiguity lobes. A jammer is evident at 5.2 degrees from broadside. An ambiguous range cell occurs at 62.5 km.

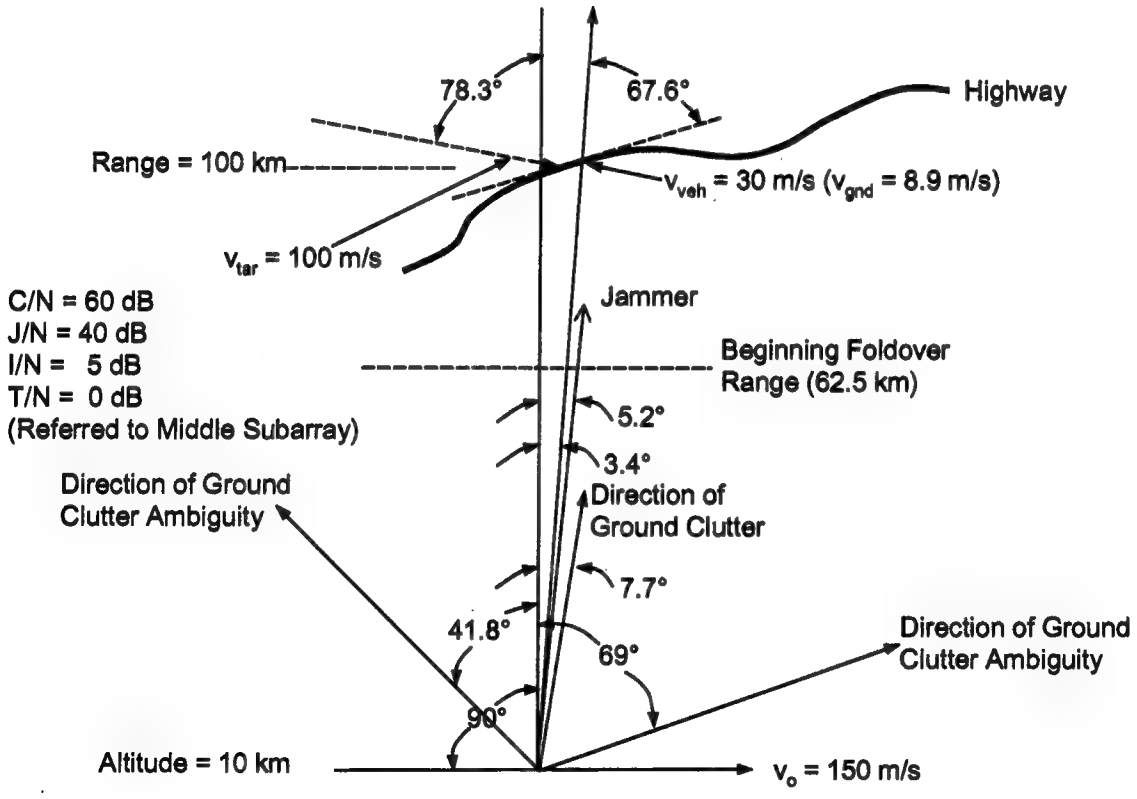

Figure 3-6: Geometry

The signal levels are adjusted so that at the middle subarray, clutter to noise ratio (*C/N*) is 60 dB, jamming to noise ratio *(J/N)* is 40 dB, highway clutter to noise ratio *(I/N)* = 5 dB, and target response to noise ratio *(T/N)* is 0 dB.

The pertinent angle/Doppler diagram is shown in Figure 3-7. Sine azimuth angle relative to beam direction sine angle is plotted vs radial velocity to beam direction ground velocity. The quiescent two way antenna pattern and Doppler filter pattern also are shown. The two-way antenna pattern is plotted as a function of clutter ridge Doppler (or equivalent radial velocity) using the well known relation between clutter angle and clutter Doppler. The apparently high near sidelobes in the two way pattern are a result of the beamwidth mismatch between the relatively broad mainlobe of the receive pattern and the narrow mainlobe of the transmit pattern. The data is replotted with a contracted velocity scale in Figure 3-8. The Doppler ambiguity lobes are now evident.

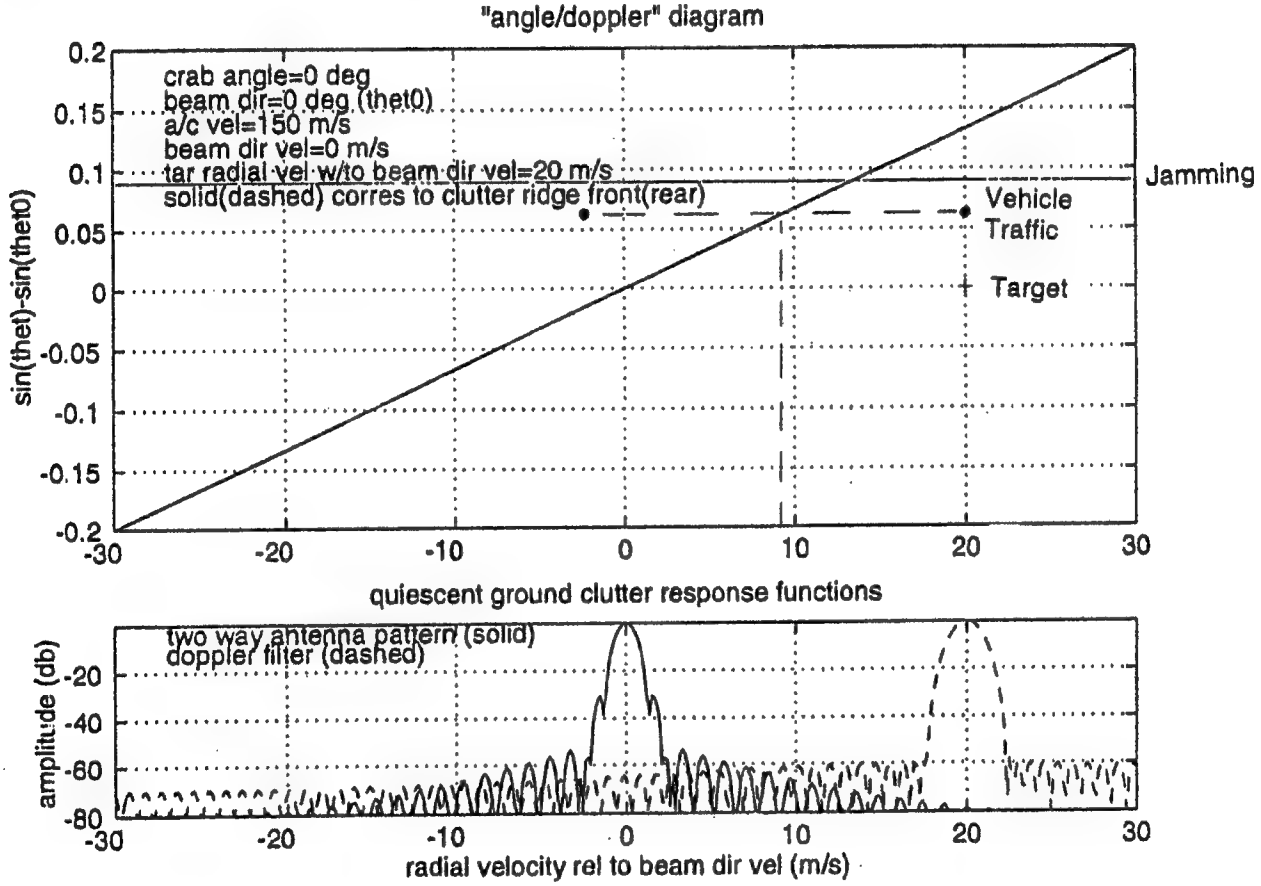

Figure 3-7: Angle/Doppler Diagram

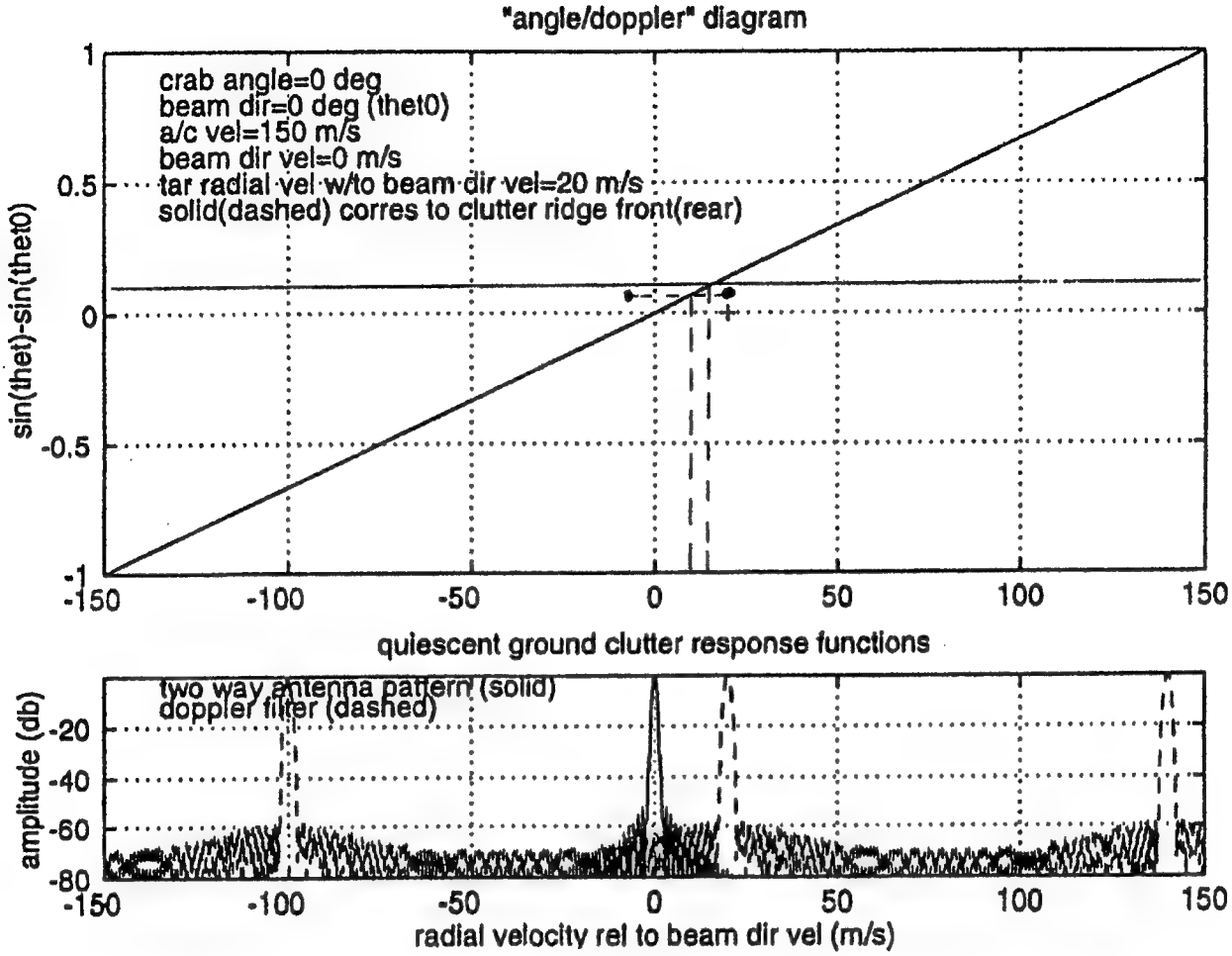

Figure 3-8: Angle/Doppler Diagram – Contracted Scale

Simulations of the radar filtering were carried out for a variety of situations. Figure 3-9 shows the results of Doppler processing (no STAP) in the absence of highway induced discretes and jamming. The only interference was ridge clutter and receiver noise. The filter amplitude output versus range and radial velocity is plotted. The lower display is a constant radial velocity cut (at the target radial velocity of 20.2 m/s). Apparently, the output SINR was only ~4.7 dB. The subsequent introduction of STAP processing increased the SINR to ~14.2 dB (Figure 3-10), but the introduction, then, of highway traffic (Figure 3-11) clearly demonstrated that low DOF STAP is ineffective against this type of clutter discretes.

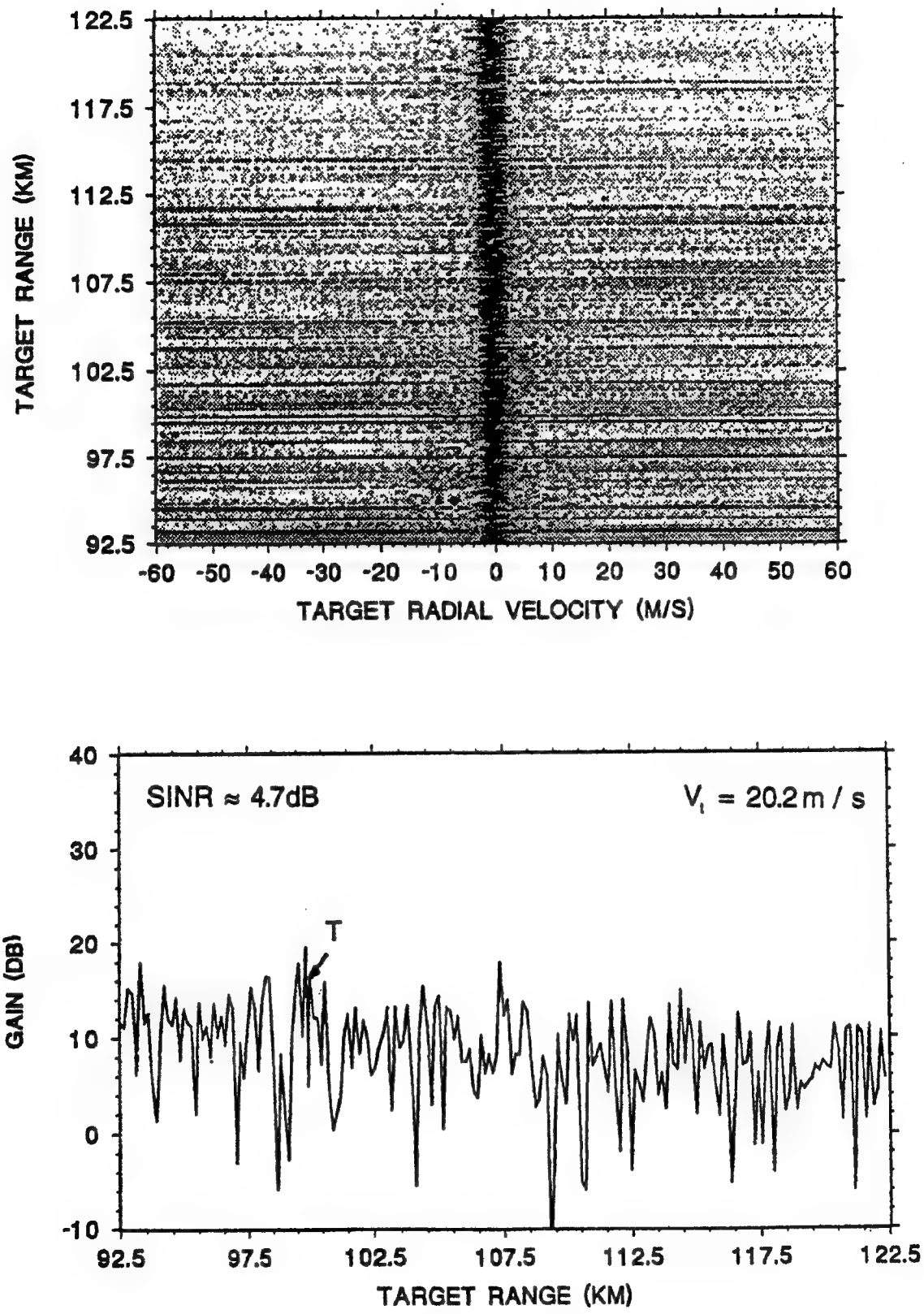

Figure 3-9: No STAP, Notching, or Adaptive Nulling; No Highway Traffic or Jamming

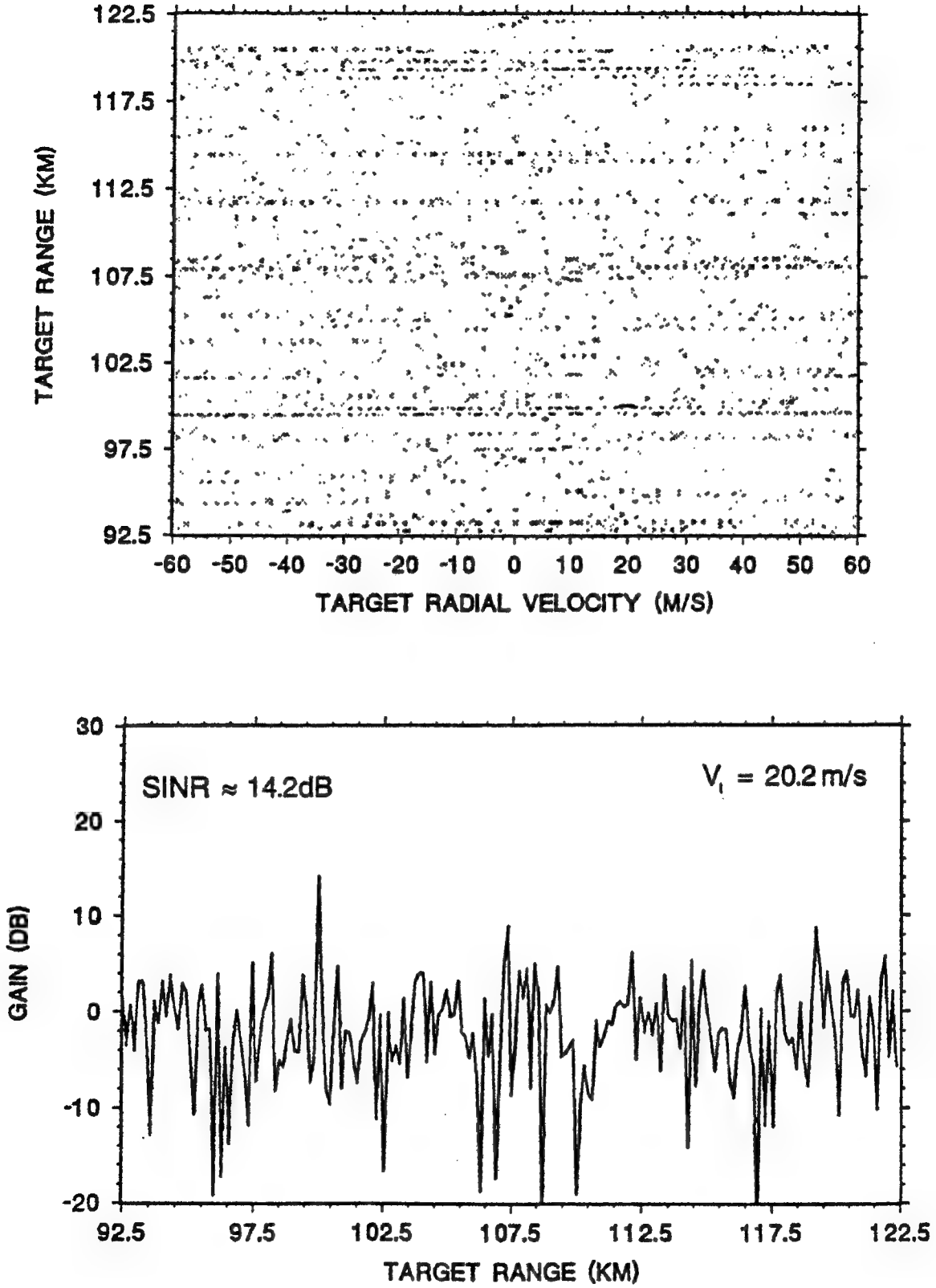

Figure 3-10: STAP only; no Highway Traffic or Jamming

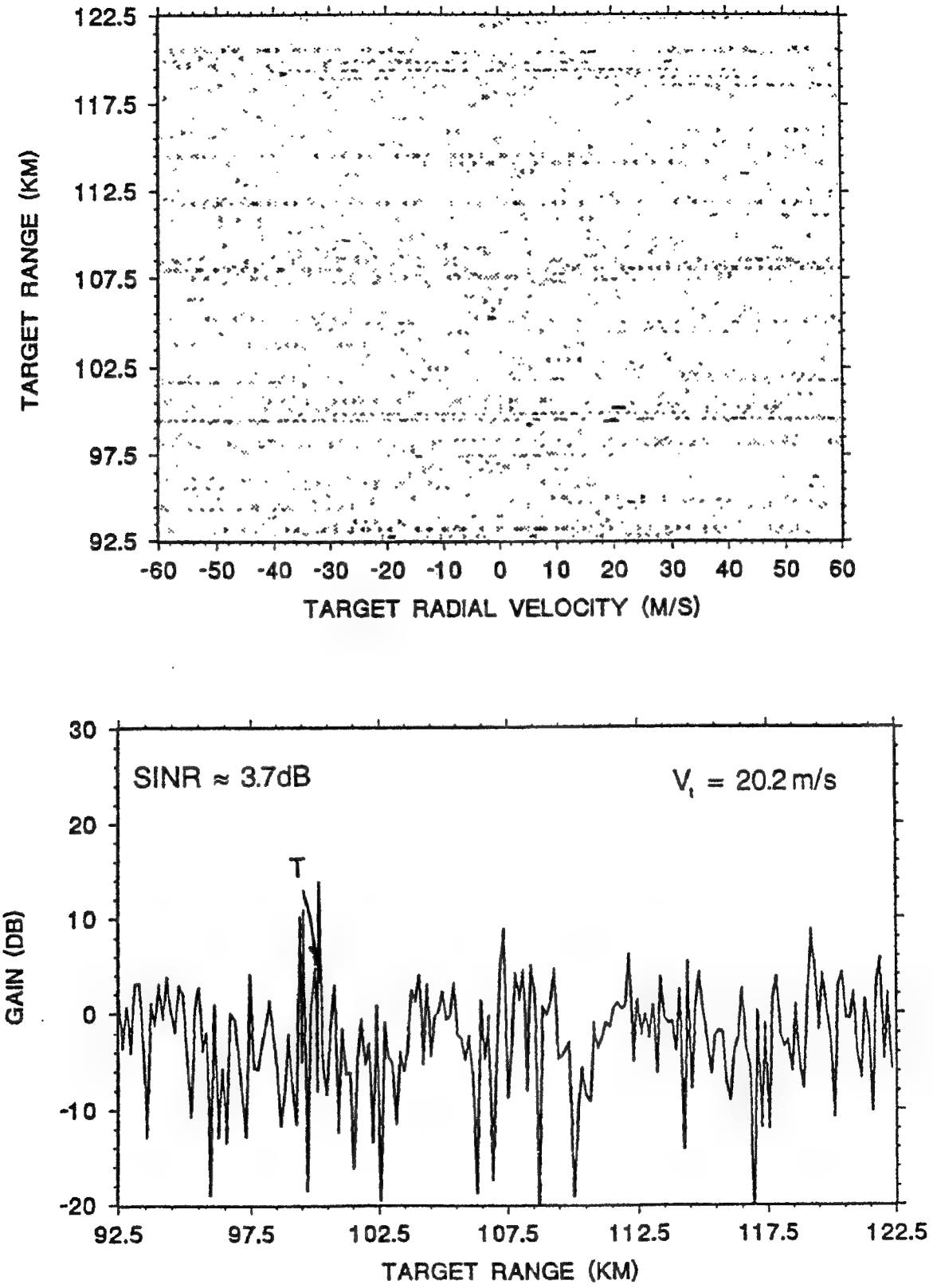

Figure 3-11: STAP Only; Highway Traffic but no Jamming

Pattern synthesis was then introduced to notch the highway clutter. Symmetric notching was applied to retain pattern symmetry in order to minimize monopulse angle measurement error. The sum and difference patterns before (solid) and after (dashed) synthesis are shown in Figure 3-12. Notching in the highway direction (3.4 degrees) is clearly evident in both patterns. The result of applying notching and STAP to suppress ridge clutter and highway discretes is shown in Figure 3-13. Clearly, the notching improved performance.

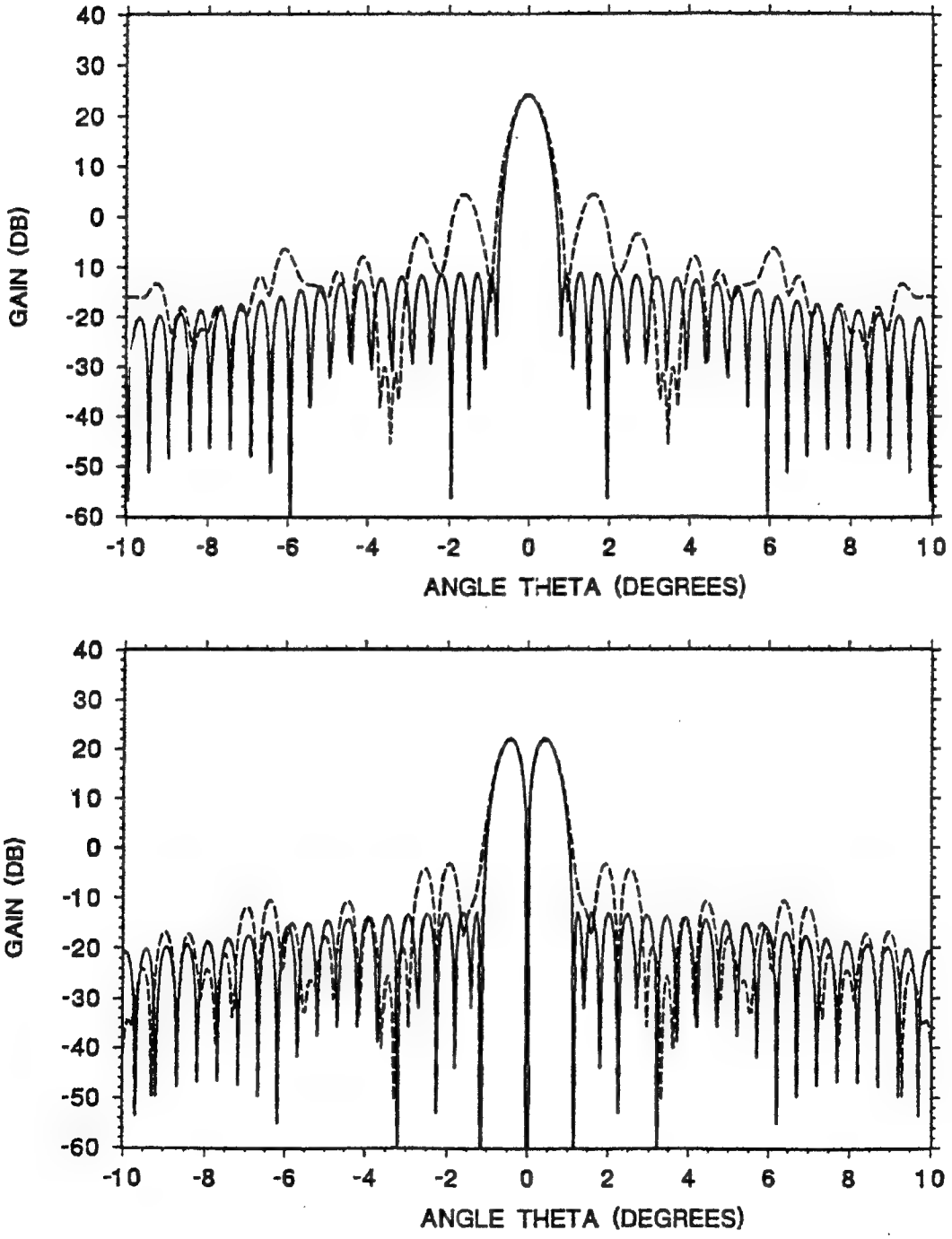

Figure 3-12: Symmetric Notched (3.2 – 3.7 Degrees) Patterns

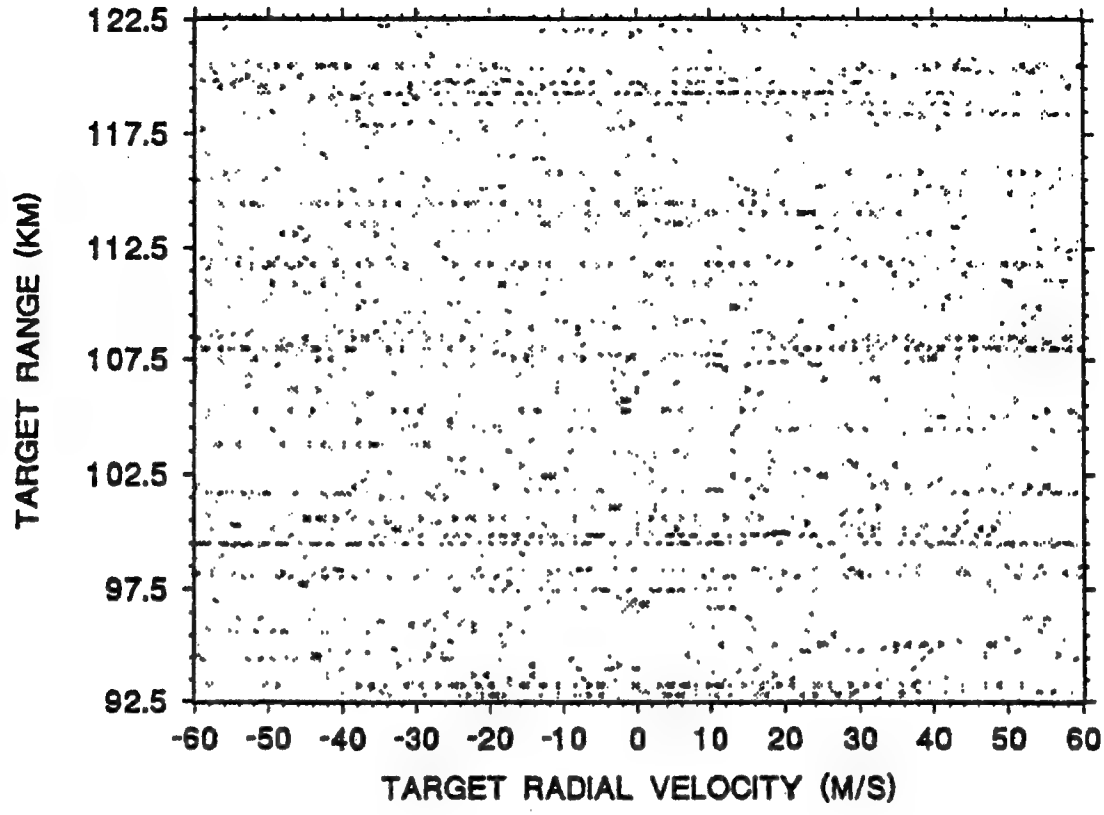

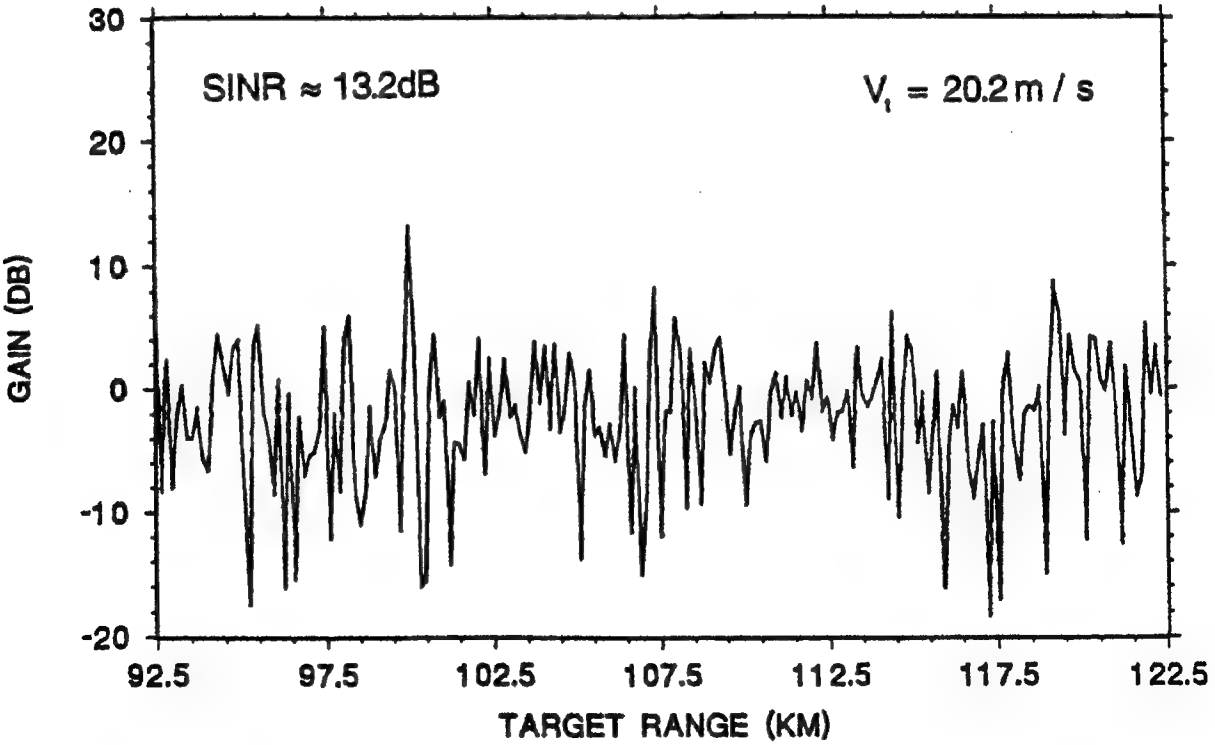

Figure 3-13: STAP and Notching; Highway Traffic but no Jamming

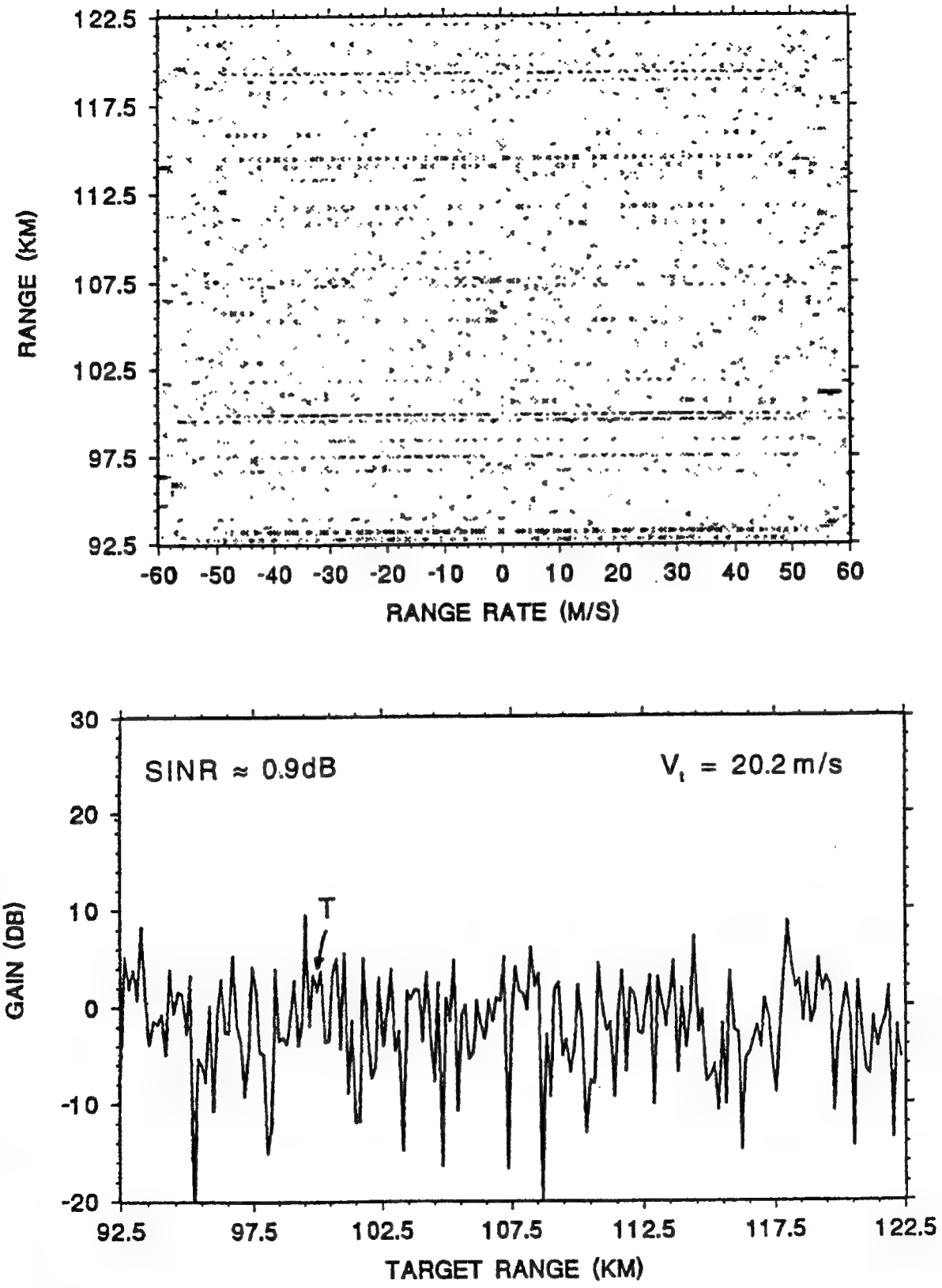

Figure 3-14: STAP and Notching; Highway Traffic and Jamming at 5.2 degrees

The introduction of jamming substantially degraded performance in spite of the low DOF STAP filtering (Figure 3-14). (The effectiveness of a large DOF method against clutter discretes and jamming is shown below.) The introduction of spatial only adaptivity to combat the jamming then was applied. The sum and difference patterns before (solid) and after (dashed) notching and spatial only adaptivity are shown in Figure 3-15. No effort was made to retain pattern symmetry in the adaptivity. Simultaneous notching in the highway direction (3.4 degrees) and jammer direction (5.2 degrees) is clearly evident in both patterns. The result of applying spatial only adaptivity, notching, and STAP to suppress ridge clutter, jamming, and highway discretes is shown in Figure 3-16. Improved performance is evident.

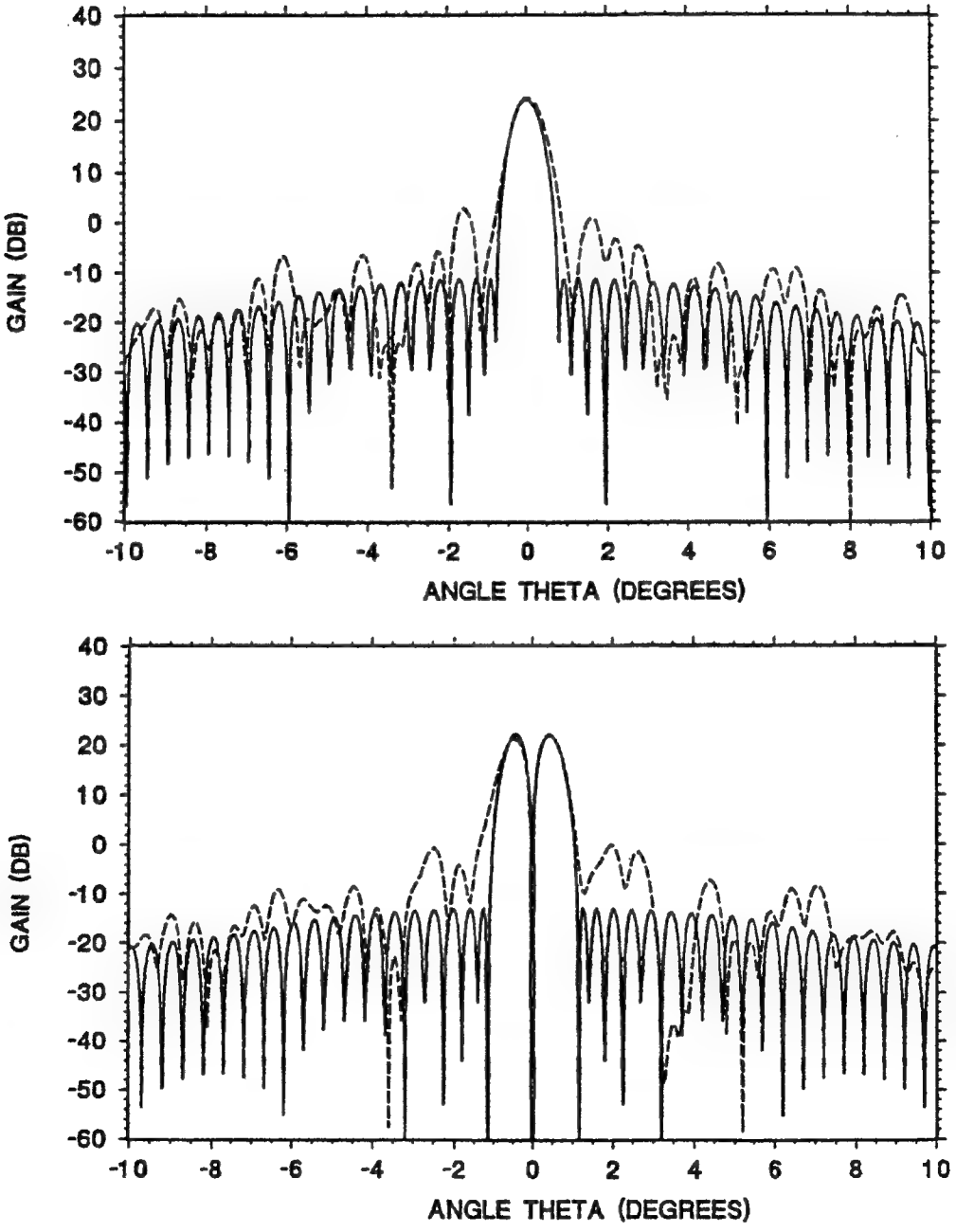

Figure 3-15: Notched and Adaptively Nulled Patterns

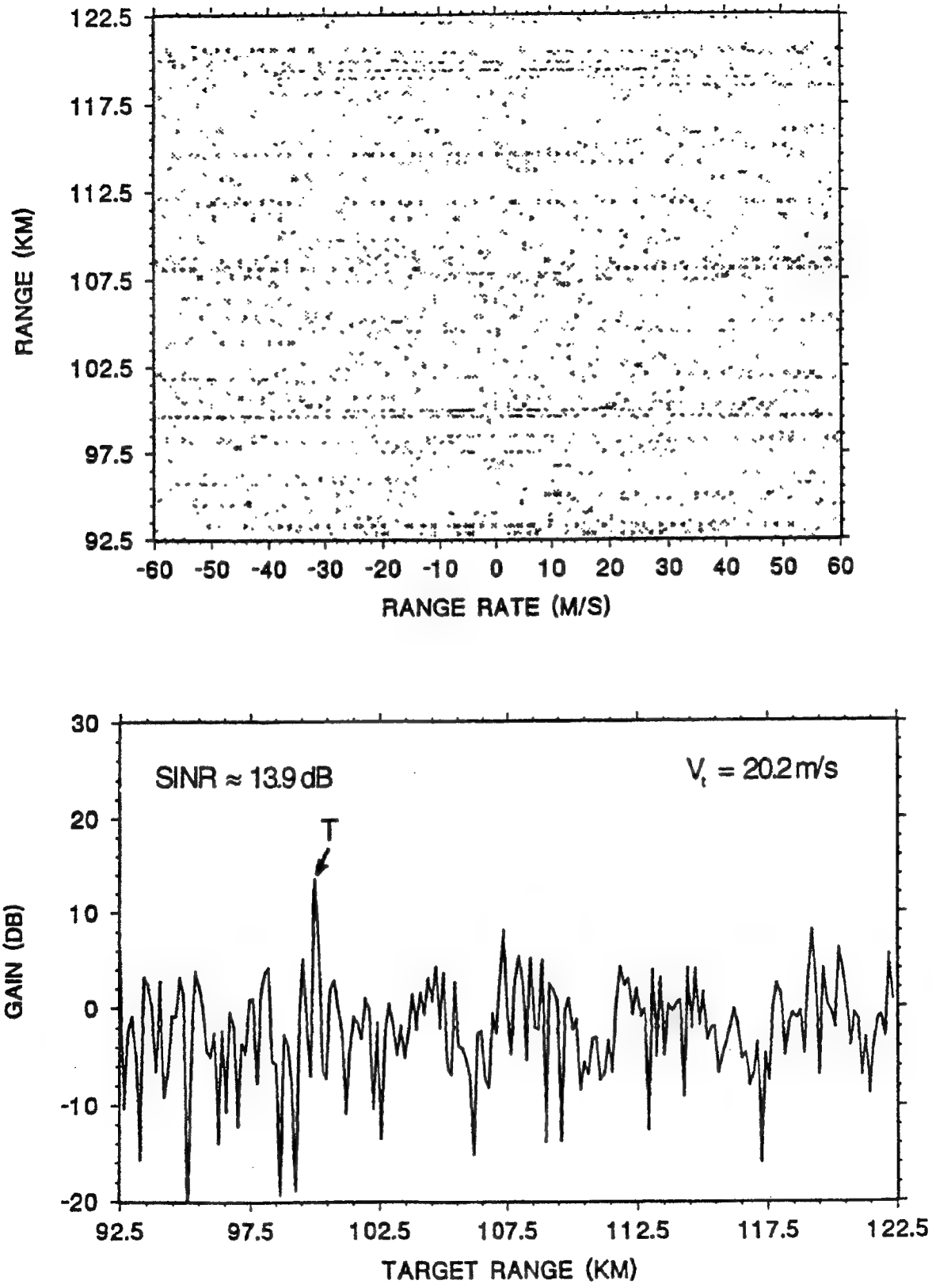

Figure 3-16: STAP, Notching, and Adaptive Nulling; Highway Traffic and Jamming

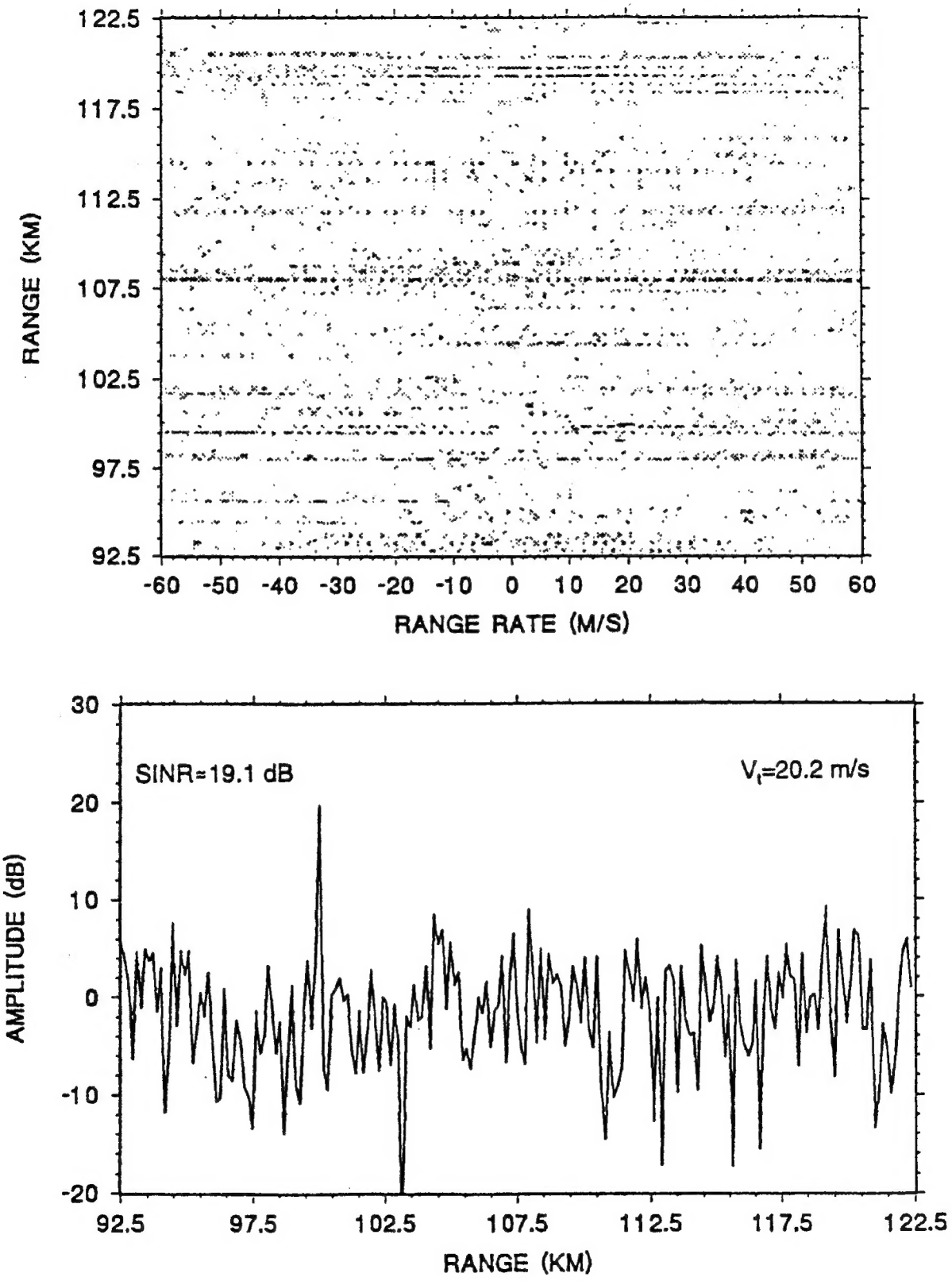

Figure 3-17: Large Degree of Freedom STAP; Jamming but no Highway Traffic

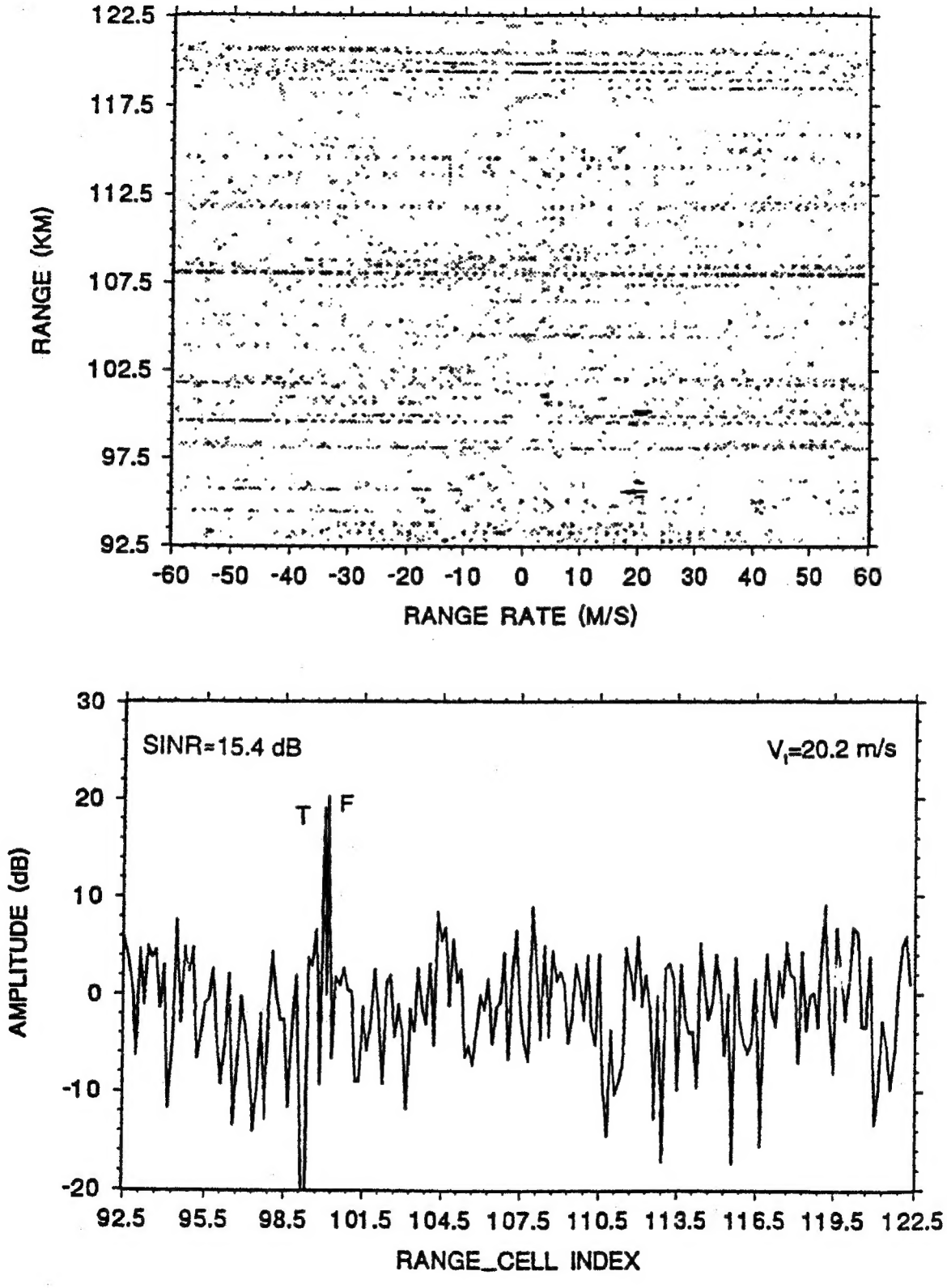

Figure 3-18: Large Degree of Freedom STAP; Jamming and Highway Traffic

The large DOF STAP configuration of Figure 3-3 was then applied to the scenario containing jamming but no highway discretes. Figure 3-17 shows the satisfactory performance that resulted. The introduction of highway discretes (Figure 3-18), however, degraded performance principally by causing a false target to appear. Notching, to suppress the discretes, could not be applied because all spatial degrees of freedom were applied in the STAP.

3.4 Conclusion

Pattern synthesis (deterministic notching) and spatial only adaptivity in combination with a small DOF STAP has been demonstrated to be advantageous in suppressing most types of interference. An alternative filtering architecture that allocates all available spatial degrees of freedom to STAP appears to work very well also, perhaps even better, except for the potential of false alarms arising from the discretes. These false alarms could be discarded by the tracking process and so are probably not a major concern. Perhaps the major benefit of deterministic notching is that it is applied with a small DOF STAP method with the associated requirement for less reference data than are required for the large DOF STAP methods. The validity of this assertion would require extensive testing with measured clutter data or detailed modeled clutter data.

Section 3.0 References

1. "Radar Filtering Rulebook," SRC RD 97-1466, Syracuse Research Corporation, Syracuse, NY, 31 October 1997.

2. E.C. Dufort, "Pattern Synthesis Based on Adaptive Array Theory," *IEEE Trans. Ants. Progp.*, vol 37, No. 8, pp 1011 – 1018, August 1989.

*U.S. GOVERNMENT PRINTING OFFICE: 2001-610-055-10148